AD NUMBER

AD073756

NEW LIMITATION CHANGE

TO

Approved for public release, distribution unlimited

FROM

Distribution authorized to DoD only; Administrative/Operational Use; APR 1955. Other requests shall be referred to Wright Air Development Center, Wright-Patterson AFB, OH 45433.

AUTHORITY

USAF HQS 88ABW, 88CG/SCCMF ltr, 17 Mar 2006

UNCLASSIFIED

AD NUMBER
AD073756
CLASSIFICATION CHANGES
TO unclassified
FROM confidential
AUTHORITY
30 Apr 1967, DoDD 5200.10

THIS PAGE IS UNCLASSIFIED

AD NUMBER
AD073756
CLASSIFICATION CHANGES
TO confidential
FROM secret
AUTHORITY
30 Apr 1958, DoDD 5200.10

AD 737 56

Armed Services Technical Information Agency

Reproduced by
DOCUMENT SERVICE CENTER
KNOTT BUILDING, DAYTON, 2, OHIO

SECRET

MX-2276

ADVANCED STRATEGIC WEAPON SYSTEM

PRELIMINARY GLOBAL SYSTEM STUDY

U.S. MILITARY UTILIZATION

CONTRACT NO. AF33(616)-2419

REPORT NO. D143-945-014

29 APRIL 1955

BELL *Aircraft* CORPORATION

JUL 29 1955

56 WC 8   8923-C-5

BELL *Aircraft* CORPORATION
BUFFALO 5.   ·   NEW YORK

TECHNICAL DATA

Prepared by ___*Krafft A. Ehricke*___
$\qquad\qquad\qquad$ Krafft A. Ehricke

REPORT NO. D143-945-014

MX-2276 ADVANCED STRATEGIC WEAPON SYSTEM

PRELIMINARY GLOBAL SYSTEM STUDY

DATE 28 April 1955

U. S. [...] TION

By _____ Date _____	**BELL** *Aircraft* CORPORATION	Model _____	Page _____
Checked _____ Date _____		Missile Airplane _____	Report **D143-945-014**

Notice: Except as hereinafter listed or marked, Bell Aircraft Corporation has no positive knowledge of the existence of other copyright, proprietary, or patent information contained in this report.

NOTICE

BELL AIRCRAFT CORPORATION reserves all
rights of whatsoever nature in and to
the developments herein described which are
claimed in issued and/or pending patents in
BELL'S name, except as any of same are or
may be licensed to the United States Govern-
ment for its use.

SECRET

By _____ Date _____ | BELL *Aircraft* CORPORATION | Model _____ Page __ii__
Checked _____ Date _____ | | Missile
 | | Airplane _____ Report D143-945-014

TABLE OF CONTENTS

SECRET

By _____ Date _____   BELL *Aircraft* CORPORATION Model _____ Page __iii__
Checked _____ Date _____   Missile
                                                                Airplane _____ Report __D143-945-014__

ILLUSTRATIONS

SECRET

By	Date	BELL Aircraft CORPORATION	Model	Page	iv
Checked	Date		Missile Airplane	Report	D143-945-014

ILLUSTRATIONS (CONT)

By _____ Date _____ | **BELL** *Aircraft* CORPORATION | Model _____ Page ____V____

Checked _____ Date _____ | Missile Airplane _____ Report D143-945-014

TABLES

Form E4-1 Rev. 353

I. ABSTRACT

Four types of global flight paths are examined and compared
with the skip path. With the latter path, a vehicle can circumnavigate
the globe without attaining circular velocity. However, for operational
reasons, it is necessary to consider flight paths involving either
circular or higher velocities. The four paths considered are a spiral
path, an elliptic path, a constrained path, and a sustained path. The
assumptions used and the methods of calculation are described in
some detail. A brief study of the weight of vehicles capable of
attaining the various flight paths is also included.

The specific requirements, advantages, and disadvantages of
each type of path have been summarized.

Form E4-1 Rev. 353

II. INTRODUCTION

The global weapon system is defined as a reconnaissance and/or bombing vehicle which completes at least one circumnavigation of the globe before descending to the surface and which, therefore, is capable of returning to its take-off site within the continental United States.

Rocket propulsion is superior to other modes of propulsion at very high speeds and altitudes. Therefore, the natural field of application of a rocket-powered weapon system lies at very high speeds approaching, or even exceeding circular velocity. The effect of frictional heating on the airframe structure imposes minimum altitude limits which bece ne higher as the flight speed increases. The aerodynamic phenomei accompanying the body motion at high speed and altitude rapidly rec ice the effectiveness of the atmosphere as a means for transportation. At the same time, inertial effects, inherently associated with curved high-speed motion about the earth's center, progressively remove the need for aerodynamic lift. Therefore, as circular velocity is approached, it is logical to utilize this centrifugal effect to gain range inertially rather than aerodynamically. It is then no longer necessary to use air for gliding. Range is obtained more efficiently under near-vacuum conditions where the drag is very small. The atmosphere gains new significance as a brake to decelerate the descending vehicle. The important difference in this case is that the descent can occur at maximum lift coefficient rather than maximum lift-over-drag ratio, as required for greatest aerodynamic range. During flight at maximum lift coefficient, range is sacrificed for the sake of maximum altitude at any given speed. The lower pressure at greater altitude effectively reduces the transport of thermal energy from the outer, hot boundary layer regions to the airframe. Therefore, this type of flight path results in a decrease of heat flux density into the skin, compared to the maximum lift-over-drag path, and alleviates the technical difficulties associated with aerodynamic heating. Another advantage in gaining range inertially rather than aerodynamically lies in the low degree of energy dissipation because the drag force is considerably smaller than in aerodynamic flight. The vehicle therefore loses relatively little energy during cruise above approximately 400,000 ft. Replacement of this energy decrement by an additional burst of power does not require much propellant and permits a second circumnavigation at negligibly small expense, compared to the effort required for the first revolution.

These three potential advantages — independence from bases outside the continental United States, alleviation of the temperature problem, and rapidly growing flight efficiency with increasing number of circumnavigations — make the global weapon system an attractive extension of the MX-2276 hypersonic weapon concept. This report summarizes the preliminary analyses of various global weapon system flight paths.

SECRET

By _____ _____ _____ Page ___4___

Checked _____ Date _____ _____ Missile _____ Airplane _____ Report D143-945-014

III. GENERAL DISCUSSION OF FLIGHT PATH TECHNIQUES

Figure 1 compares different flight path techniques available
to rocket-powered intercontinental weapon systems in order to
illustrate the relative position of the global weapon system. The
ballistic trajectory for 5,000 nautical mile-range with initial velocity
of 23,000 feet per second, leads to an altitude of the order of 700
nautical miles, or, 4.2 million feet. For the same initial velocity,
the range can be increased to about 12,000 nautical miles by using a
glide path. Considerably lower altitudes, not exceeding 250,000 feet,
are required for this path. Although strongly influenced by the
centrifugal effect, this flight path retains its aerodynamic character
because lift and aerodynamic control are always needed. An optimistic
estimate indicates that a further increase in range to about 19,500
nautical miles at the same initial velocity, can be obtained by using
the skip path concept, which actually combines the ballistic flight path
with the glide path. The maximum altitude of this path can be expected
to lie between the altitudes found for the two previously mentioned
paths. In the present case, the first "peak" leads the vehicle to nearly
950,000 feet altitude, followed by a "valley" at about 250,000 feet
altitude, which is reached approximately 480 seconds after passing
the first peak. In this valley the normal load factor, which is zero
during the ballistic portion of the path, reaches a value of about 6.5g
absolute. Weightlessness is restored while climbing to the second
peak (about 625,000 feet altitude). In the second valley the normal
load factor is 3.5g absolute. With each subsequent valley the normal
load factor becomes smaller. However, in the fifth and sixth valleys
it is still of the order of 2.3g absolute. The sixth valley is passed
nearly 3000 seconds (50 minutes) after reaching the first peak. By
that time the vehicle has covered a range of about 11,500 nautical miles
and its velocity has been reduced to 19,000 feet per second. There-
after, the normal load factor decreases rapidly below 1g at all times,
because the upwardly directed centrifugal acceleration due to the
flight speed (which still remains high) more than compensates for the
small increase in apparent weight in the now rather flat valleys. At
about 13,500 nautical miles from the take-off point, the decay into a
glide path is practically completed. The velocity is 18,000 feet per
second, and, with this residual energy, the vehicle is capable of adding
another 6,000 nautical miles to bring the total range to 19,500 nautical
miles. This is not a full circumnavigation of the globe, but a path of
this length will permit the location of the landing site within an area
covering the continental United States or its immediate vicinity. In

BALLISTIC PATH
ELLIPTIC PATH
SKIP PATH
GLIDE PATH

Figure 1. Comparison of Flight Path Techniques

terms of range for a given initial speed the skip path is most effective. However, extremely accurate flight control is required, in order to accomplish the frequent transitions from vacuum to atmospheric flight. A dual control system is needed — jet control for vacuum and aerodynamic control for the atmospheric portion. These systems have to be activated alternately while maintaining the attitude angle of the vehicle with a degree of accuracy which would be difficult to accomplish even in the simpler case of only one control system continuously in operation. A slight error in the angle of attack, particularly in the first valleys, would significantly alter the flight path and produce normal load factors much in excess of the high values already experienced along the correct path. These load factors and the addition of adequate safety factors for the pilot would lead to a considerably higher take-off weight for the same cut-off velocity than in either the ballistic or the glide case. This weight penalty alone offsets much, if not all, of the range advantage associated with the skip path. A final principal disadvantage of the skip path is that it is not well suited for reconnaissance missions because of the frequent altitude variations and is even less suitable for bombing because of simultaneous and continuous changes in altitude, velocity, and trajectory angle.

IV. DESCRIPTIONS OF FLIGHT PATHS FOR THE GLOBAL WEAPON SYSTEMS

Although from the viewpoint of flight mechanics alone, the skip path can lend global capacity to a vehicle not capable of attaining circular speed, it is necessary for operational reasons to consider other flight paths on a higher level of energy which involve circular or even higher flight velocities. These paths (discussed in Sections IV through VII) are the spiral path, the elliptic path, and the constrained path. Only the elliptic path, which involves comparatively the greatest variation in altitude, is shown in Figure 1 for the sake of clarity. In addition to these three flight path types, a fourth possibility has been explored — the sustained path (Section VIII) which involves motion at constant velocity and constant altitude by means of a sustainer rocket motor. In order to avoid excessive mass consumption while following the sustained path, the drag must be small, which requires high altitude and consequently high flight speed, probably approaching or reaching circular velocity.

The three flight paths, spiral, elliptic, and constrained, are depicted in Figures 2 through 4 together with some characteristic data of each path.

Path I (Spiral)

As shown in Figure 2, the vehicle is delivered horizontally at circular speed at an altitude sufficient to complete one circumnavigation of the globe. The vehicle remains in the atmosphere and loses speed throughout the cruise. The resulting flight path is a spiral. When entering the denser atmosphere, the aerodynamic portion of the flight occurs at maximum lift coefficient rather than at maximum lift-over-drag ratio. The take-off preferably occurs in the direction opposite to the shortest great circle route to the target area, because the vehicle then appears over the target area at a velocity and altitude comparable to that of the MX-2276. If more than one revolution is desired, the initial altitude must be increased. In this case the vehicle makes all passes over the target area — except the last one, at near-circular velocity and at an altitude which is considerably higher than in the case of MX-2276.
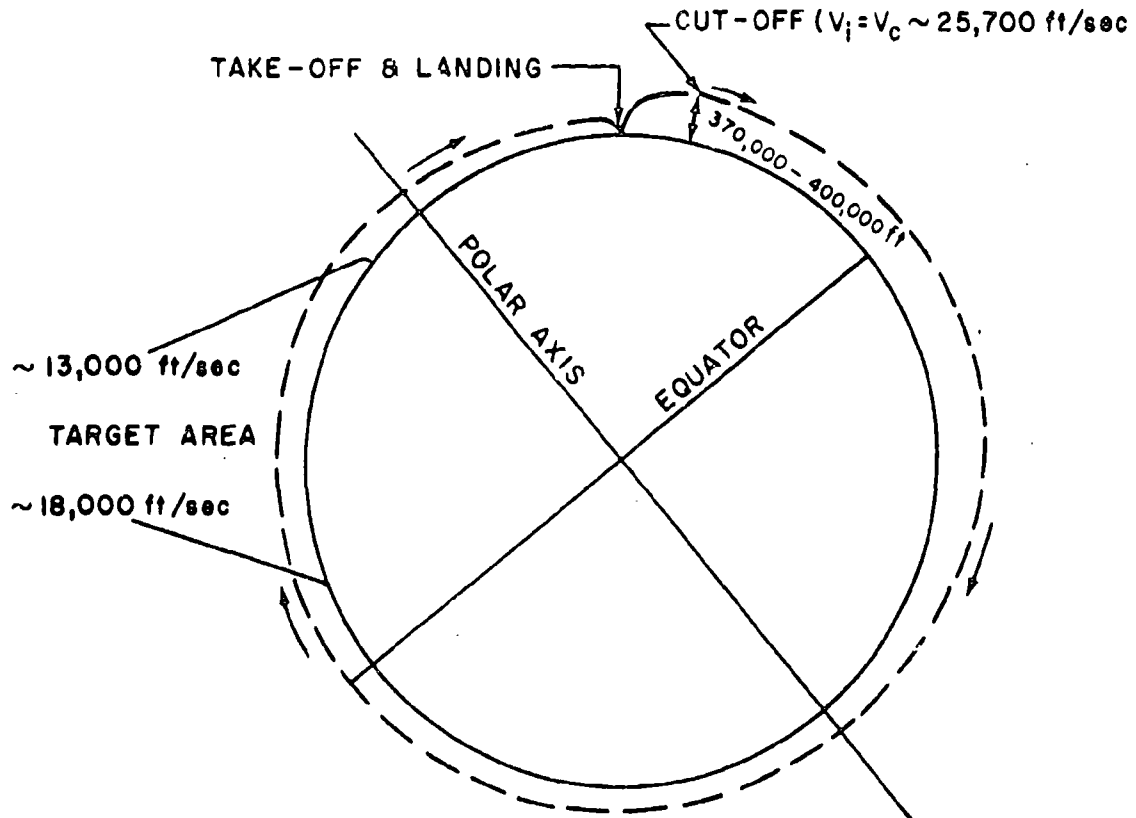
Figure 2. Path Type I: Horizontal Delivery at Circular Velocity; One
Circumnavigation; Spiral of Descent, Not Necessarily at L/D_{max}

CUT-OFF $(0.9\,V_c \lesssim V_i \lesssim V_c;\ \theta \sim 3° - 5°)$

TAKE-OFF & LANDING

SMALL IMPULSE $(\Delta V \approx 1600\ \text{ft/sec})$

θ

$y_i \sim 300,000$ ft

y_{oo}

APOGEE

POLAR AXIS

MAJOR AXIS

EQUATOR

$y_A \sim 140 - 200$ MI

$\sim 20,000$ ft/sec

TARGET AREA

NEW ELLIPSE (ECCENTRICITY < 0.02)

$\sim 25,000$ ft/sec

$y_p = 250,000 - 300,000$ ft

PERIGEE

$V_p \lesssim 26,000$ ft/sec (A SMALL VELOCITY INCREMENT, $\Delta V \cong 200 - 300$ ft/sec, PERMITS SECOND CIRCUMNAVIGATION)
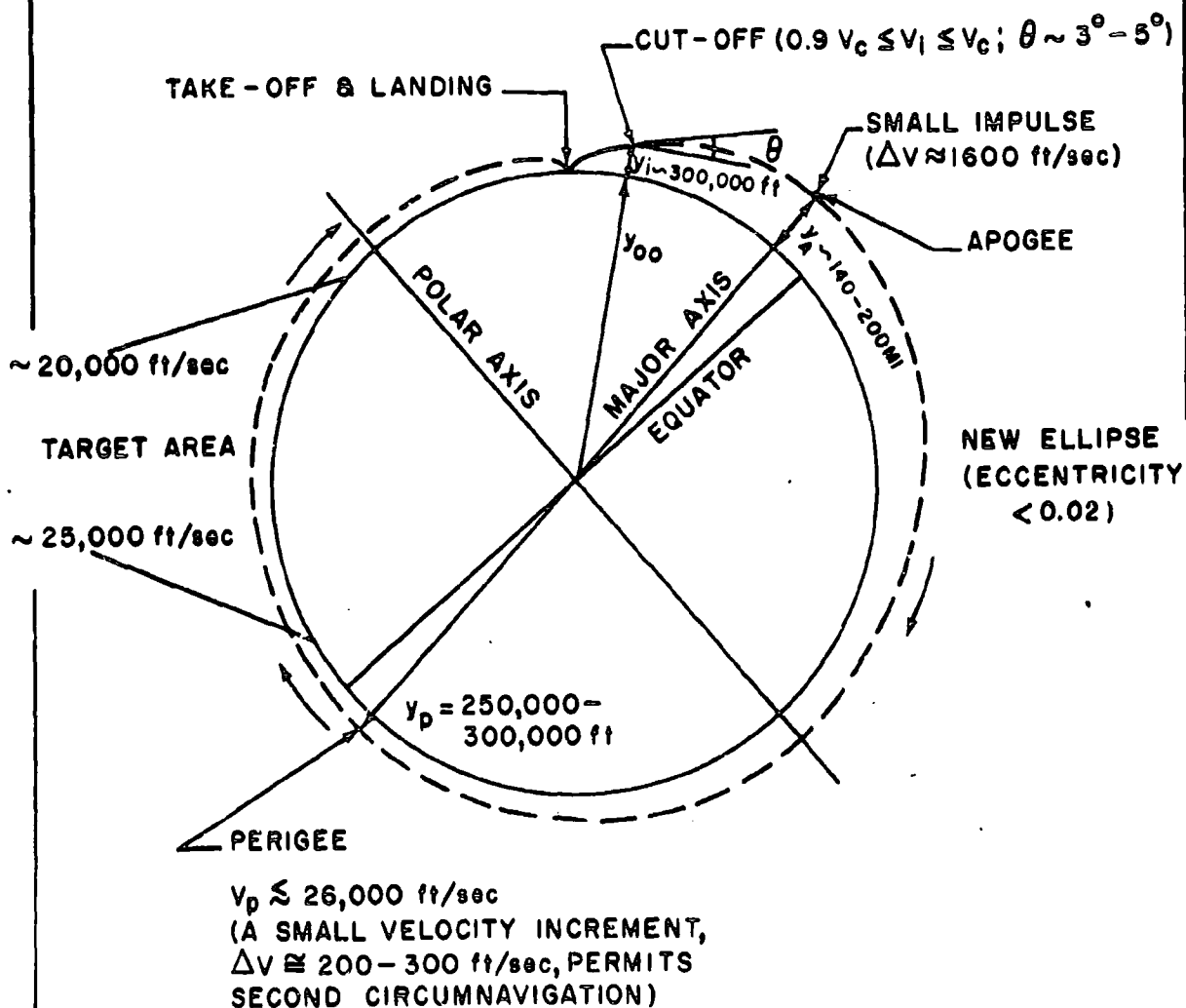
Figure 3. Path Type II: Low Eccentricity Ellipse with Perigee Near Target Area

By _____ Date _____

Checked _____ Date _____

BELL *Aircraft* CORPORATION

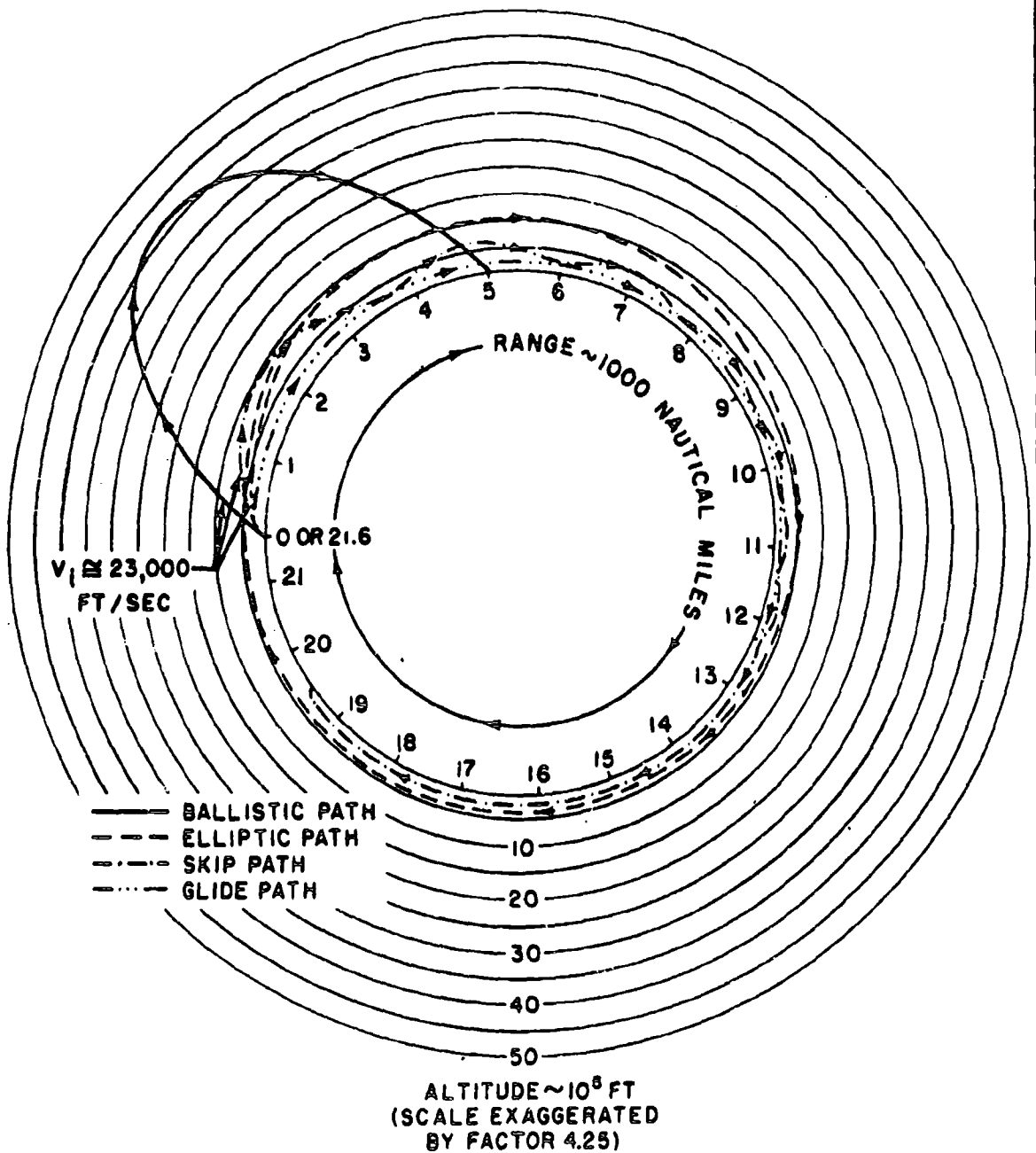Model _____ Page 10

Missile
Airplane _____ Report D143-945-014

CUT-OFF ($V_i \sim 29{,}000$ ft/sec, $y_i \sim 300{,}000$ ft)

TAKE-OFF & LANDING

POLAR AXIS

EQUATOR

$V \sim 26{,}000$ ft/sec

TARGET AREA

END OF
CONSTRAINED
PATH
($y =$ CONST.)

$V \sim 25{,}000$ ft/sec
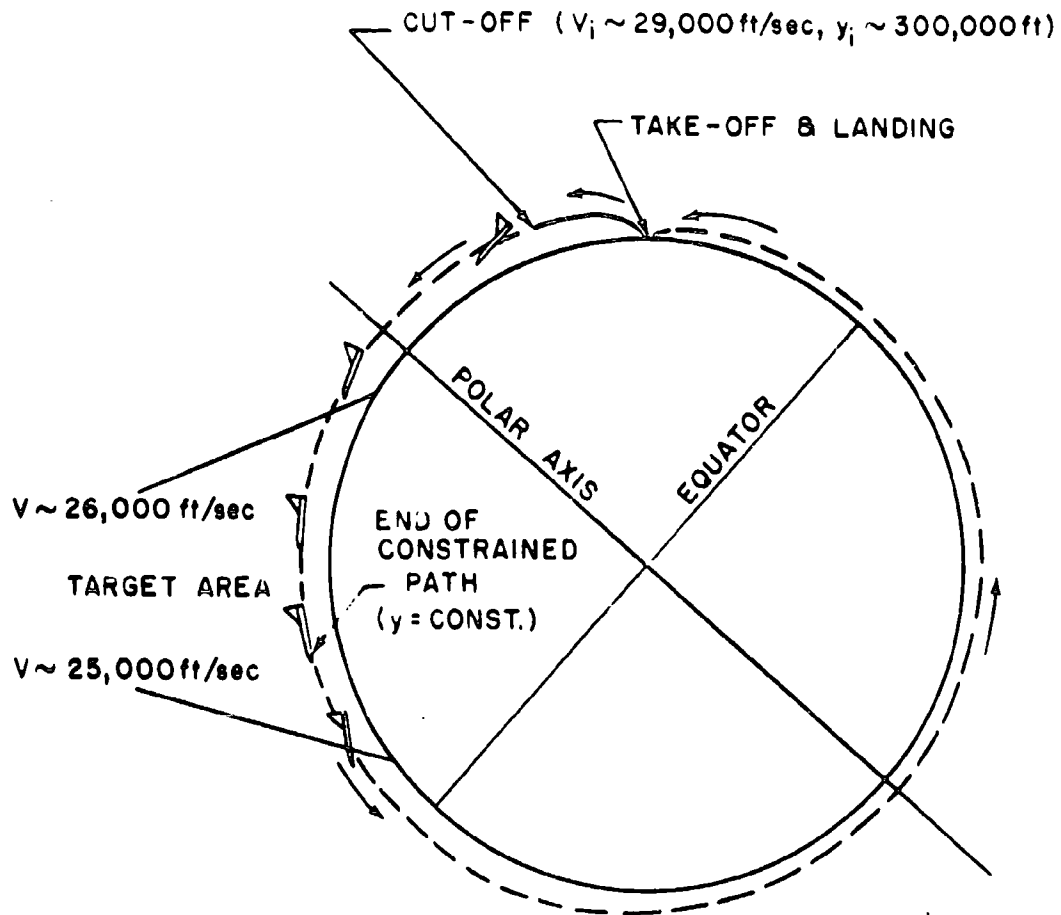
Figure 4. Path Type III: Constrained Path

Path II (Eiliptic)

The vehicle is delivered not horizontally, but at a small trajectory angle at near-circular or circular velocity (Figure 3). The resulting free flight path is an ellipse whose apogee lies above the atmosphere, but whose perigee would lie inside the earth if the vehicle were permitted to follow this path beyond the apogee. Therefore, a small impulse (burst of power) is needed so that the vehicle can enter a new ellipse whose perigee lies at an altitude of about 300,000 feet. The orientation of the major axis of the ellipse with respect to the polar axis of the earth must be such that the perigee lies over the target area. This again requires a take-off in the direction opposite to the shortest great circle route so that the far-out apogee is passed over friendly or neutral territory. Since most of the elliptic path is outside the relevant atmosphere, the velocity loss between cut-off and perigee is small, and a second circumnavigation can be effected with comparatively little additional energy. In contrast to the spiral, the ellipse enables the vehicle to appear over the target area always at about the same altitude of approximately 300,000 feet, independent of the number of revolutions. The velocity is always close to circular.

Path III (Constrained)

As shown in Figure 4, the vehicle is delivered horizontally at a cut-off speed which exceeds the local circular velocity. The excess, referred to as elliptical excess, sends the vehicle into an elliptic orbit unless it is forced, by negative lift, to stay at the initial altitude and to follow a circular path. In order to accomplish this, the vehicle must initially fly at a negative angle of attack, and the initial altitude must be low enough to permit action of a sufficiently strong aerodynamic force. The angle of attack becomes zero as the speed is reduced to circular velocity. Thereafter the path is similar to the spiral (Path I).

Path IV (Sustained)

Again the vehicle is delivered horizontally. Cut-off speed is sustained at constant altitude by a small sustainer rocket motor which overcomes the comparatively low drag.

V. PATH TYPE I: SPIRAL

The spiral path involves the comparatively smallest amount of changes from the present MX-2276 hypersonic weapon system, especially if only one circunmavigation is involved. It represents an increase in flight speed and initial altitude over the corresponding MX-2276 values. Over a considerable range the vehicle follows an inertial path of very gradual velocity reduction. The lift-over-drag ratio in the free molecule flow in which the vehicle must operate is very small (less than unity), because the lift is negligibly small while the drag is considerably larger. This increase in drag force results from the fact that, in the absence of a boundary layer, each molecule enters into a direct energy change with the wall rather than dissipating its energy in the boundary layer which acts as a cushion in transfer- ring energy from the free stream to the wall. The free-molecule flow region is therefore extremely unfavorable to aerodynamic flight. On the other hand, although the drag coefficient C_D is high in free mole- cule flow, the drag force as such is small, owing to the extremely low density. The deceleration of the vehicle is therefore correspondingly small, if the initial altitude is sufficiently high. Using circular velocity, in order to be independent of aerodynamic lift, makes it possible there- fore, to maintain very high speed over a sufficiently long time period to circumnavigate a significant portion of the earth's circumference before returning to the denser atmosphere.

The mechanics of transition from such inertial flight back to aerodynamic flight is not known at present, nor can it be determined accurately because of lack of theoretical and experimental information. It is apparent, however, that, in regions where the lift-over-drag ratio is less than 1, there will be little difference in the motion of a winged vehicle compared to a nonwinged or ballistic configuration. A real difference in flight path will not develop until the aerodynamic lift force has become sufficiently strong to make the presence or absence of a large lifting area significant. This zone of beginning aerodynamic flight will be discussed subsequently.

Figure 5 shows the density-altitude relationship and different dynamic pressures for a velocity which is approximately equal to the circular velocity in the altitude range under consideration. The density values are taken from References 1 and 2. The NACA values are based on the inverse square variation of the gravitational force. In Figure 6 the dynamic pressure is plotted versus altitude for the same speed.

Form F4-1 Rev. 353

SECRET

FIGURE 5 DENSITY RATIO VS. ALTITUDE AND TYPICAL DYNAMIC PRESSURES AT V = 25,800 FT./SEC.
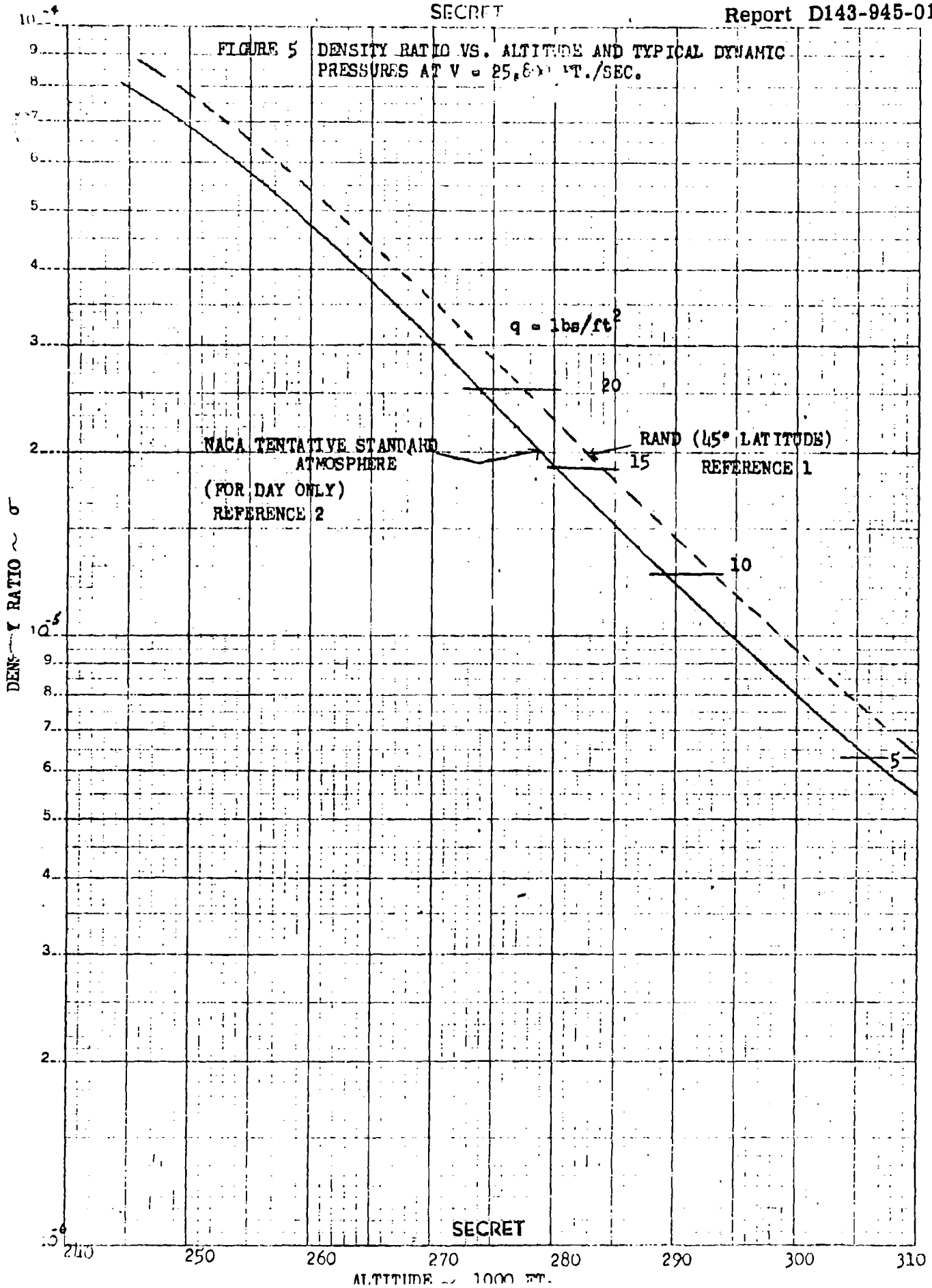
FIGURE 6 - INITIAL ALTITUDE AS FUNCTION OF DYNAMIC PRESSURE
AT ZERO ANGLE OF ATTACK ($V = V_o = 25,800$ ft./sec.)
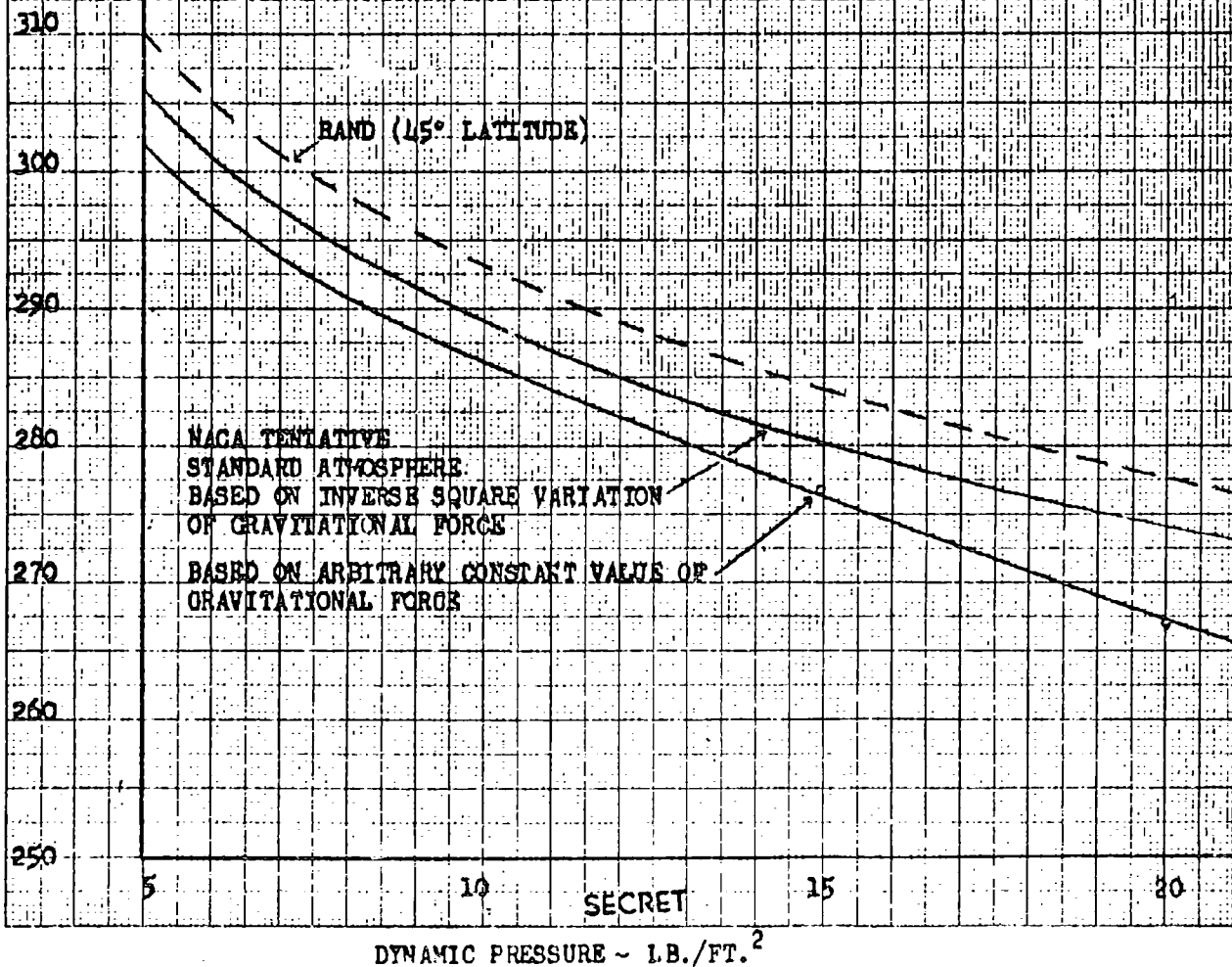
RAND (45° LATITUDE)

NACA TENTATIVE
STANDARD ATMOSPHERE
BASED ON INVERSE SQUARE VARIATION
OF GRAVITATIONAL FORCE

BASED ON ARBITRARY CONSTANT VALUE OF
GRAVITATIONAL FORCE

ALTITUDE ~ 1000 FT.

DYNAMIC PRESSURE ~ LB./FT.^{2}

This graph includes also the density data of Reference 2, based on an arbitrary constant value of the gravitational force. Because the RAND atmosphere requires the greatest altitude to obtain a given dynamic pressure and therefore yields the most conservative results for powered ascent, the altitude-density relation of Reference 1 will be used in the subsequent considerations.

The dynamic pressure as function of flight velocity is shown in Figure 7 for different altitudes. It can be seen that at a velocity of 24,000 feet per second and an altitude of 290,000 feet, a dynamic pressure of 10 pounds per square foot is obtained. This pressure is regarded by NACA as approximate minimum value for maintaining aerodynamic controllability of the vehicle.

Of primary importance for the beginning of aerodynamic flight, however, is the equilibrium glide condition according to which the lift force must be equal to the instantaneous apparent weight. The apparent weight is given by

$$W_{app} = W - F_c = W \left(1 - \frac{v^2 r}{\gamma}\right) \quad - - - - - - - - - - - - - - (1)$$

where W is the true weight at rest, F_c is the centrifugal force, v the instantaneous flight velocity, $r = r_{oo} + y$ the instantaneous distance from the center of the earth and $\gamma = gr^2 = 1.4055 \times 10^{16}$ ft^3/sec^2, a constant of the terrestrial gravity field (gravity parameter). Thus

$$L = C_L S \frac{\rho_{oo}}{2} \sigma v^2 = W \left(1 - \frac{v^2 r}{\gamma}\right) \quad - - - - - - - - - - - (2)$$

where L is the lift, C_L the lift coefficient with reference to the lifting area, S the lifting area and $\sigma = \rho / \rho_{oo}$ the ratio of density at altitude y to surface density. Solving for σ yields a measure for the instantaneous altitude

$$\sigma = \frac{W}{S} \frac{2}{C_L \rho_{oo} \gamma} \left(\frac{\gamma}{v^2} - r\right) \quad - - - - - - - - - - - - (3)$$

SECRET

FIGURE 7 DYNAMIC PRESSURE VS. VELOCITY FOR DIFFERENT ALTITUDES
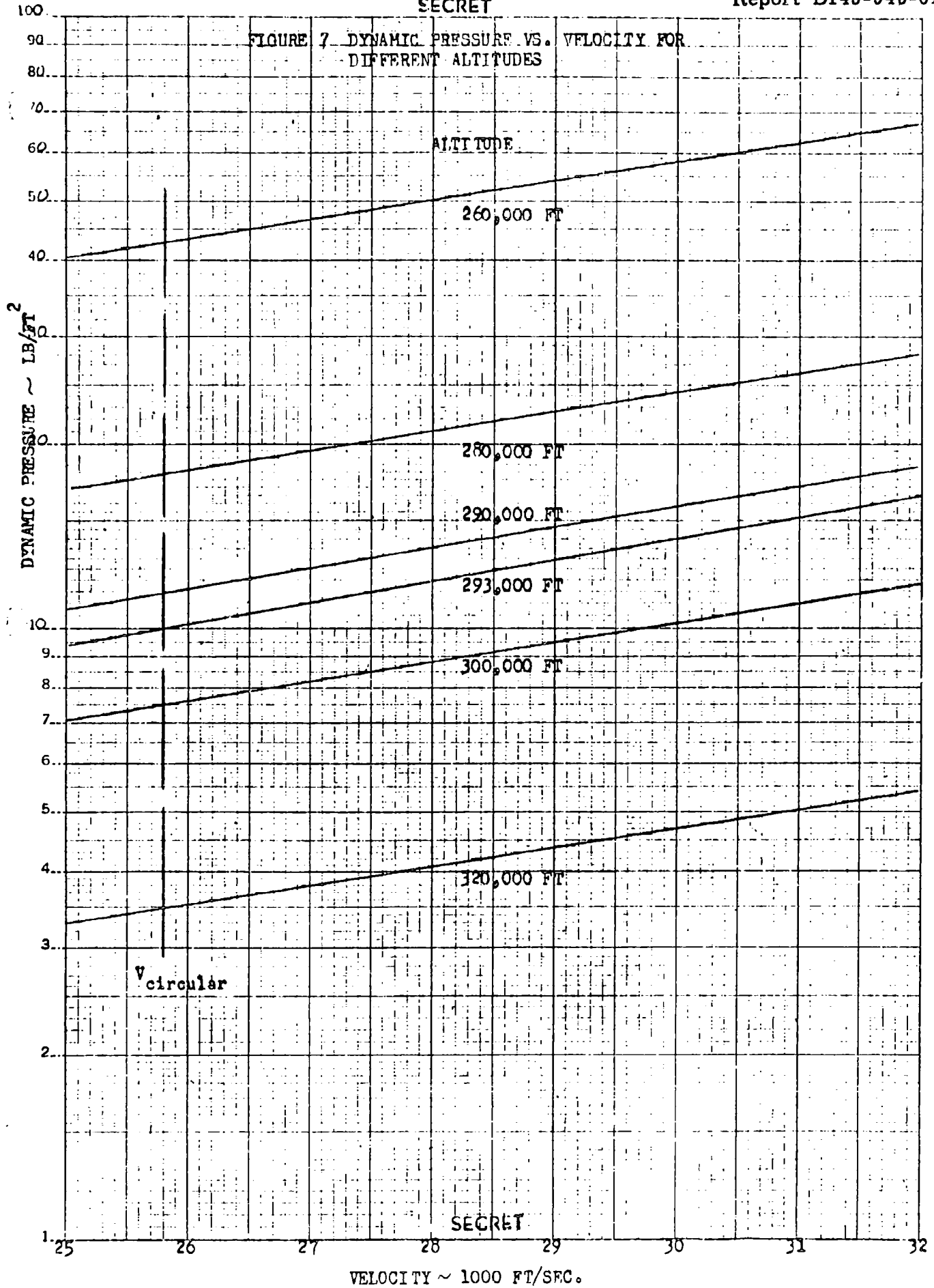
ALTITUDE

260,000 FT

280,000 FT

290,000 FT

293,000 FT

300,000 FT

320,000 FT

$V_{circular}$

DYNAMIC PRESSURE ~ LB/FT^2

VELOCITY ~ 1000 FT/SEC.

Introducing the general glide parameter $\sigma\, C_L/(W/S)$, using ρ_{oo} = 2.378 x 10^{-3} slugs per cubic foot so that $\rho_{oo}\gamma$ = 3.34228 x 10^{13} pounds per foot, and finally approximating $y/r_{oo} \sim 0$, one obtains

$$\sigma\, \frac{C_L}{W/S} = 6 \times 10^{-14} \left(\frac{\gamma}{v^2} - r_{oo} \right) \quad - - - - - - - - - - - - \quad (4)$$

so that the glide parameter is a function of the velocity only. The technically important parameter is now the ratio of lift coefficient over lifting area loss which shall be designated as the lift parameter. For a given velocity v, the right hand side of Equation (4) is known and hence, y depends solely on the lift parameter. Figures 8, 9, 10, and 11 show the change in equilibrium altitude for a number of flight velocities (both larger and smaller than circular velocity) as function of the lift coefficient, based on a true lifting area load W/S of 10, 15, 20, and 25 pounds per square foot, respectively. It can be seen that for W/S as low as 15 pounds per square foot a lift coefficient of about 0.225 is required in order to maintain an equilibrium altitude of 290,000 feet (σ = 1.4 x 10^{-5}) at a velocity of 24,000 feet per second. This is a very high value which probably cannot be obtained. Assuming C_L = 0.1, σ becomes 3.1 x 10^{-5}, corresponding to 272,000 feet. For W/S = 20, σ becomes 4.1 x 10^{-5} at v = 24,000 feet per second and C_L = 0.1 corresponding to an altitude of 266,000 feet. Conversely, at C_L = 0.1 and y = 300,000 feet, a velocity of 25,200 feet per second is required if W/S = 15, and of about 25,400 feet per second if W/S = 20. The velocity difference is small in this case because of the rapidly growing centrifugal effect as circular velocity is approached. From this it can be concluded that the vehicle, when it is slowed down to 25,000 feet per second, will have descended to the 300,000 foot level. Further deceleration to 24,000 feet per second will decrease the altitude to approximately 270,000 feet.

The altitude range which marks the beginning of aerodynamic flight, hence the beginning of a significant deviation from the path of a nonwinged vehicle will therefore be approximately 200,000 to 300,000 feet. The velocity at the beginning of aerodynamic flight is then of the order of 25,000 feet per second or slightly less.

Figure 12, which is based on Figure 17 of Reference 4, shows that for an initial velocity of 25,000 feet per second the glide range is of the order of 17,500 nautical miles, based on maximum lift/drag

FIG. 8 EQUILIBRIUM DENSITY RATIO AT VARIOUS
FLIGHT VELOCITIES AS A FUNCTION OF LIFT
COEFFICIENT FOR A WING LOADING OF 10 lb/ft.^{2}
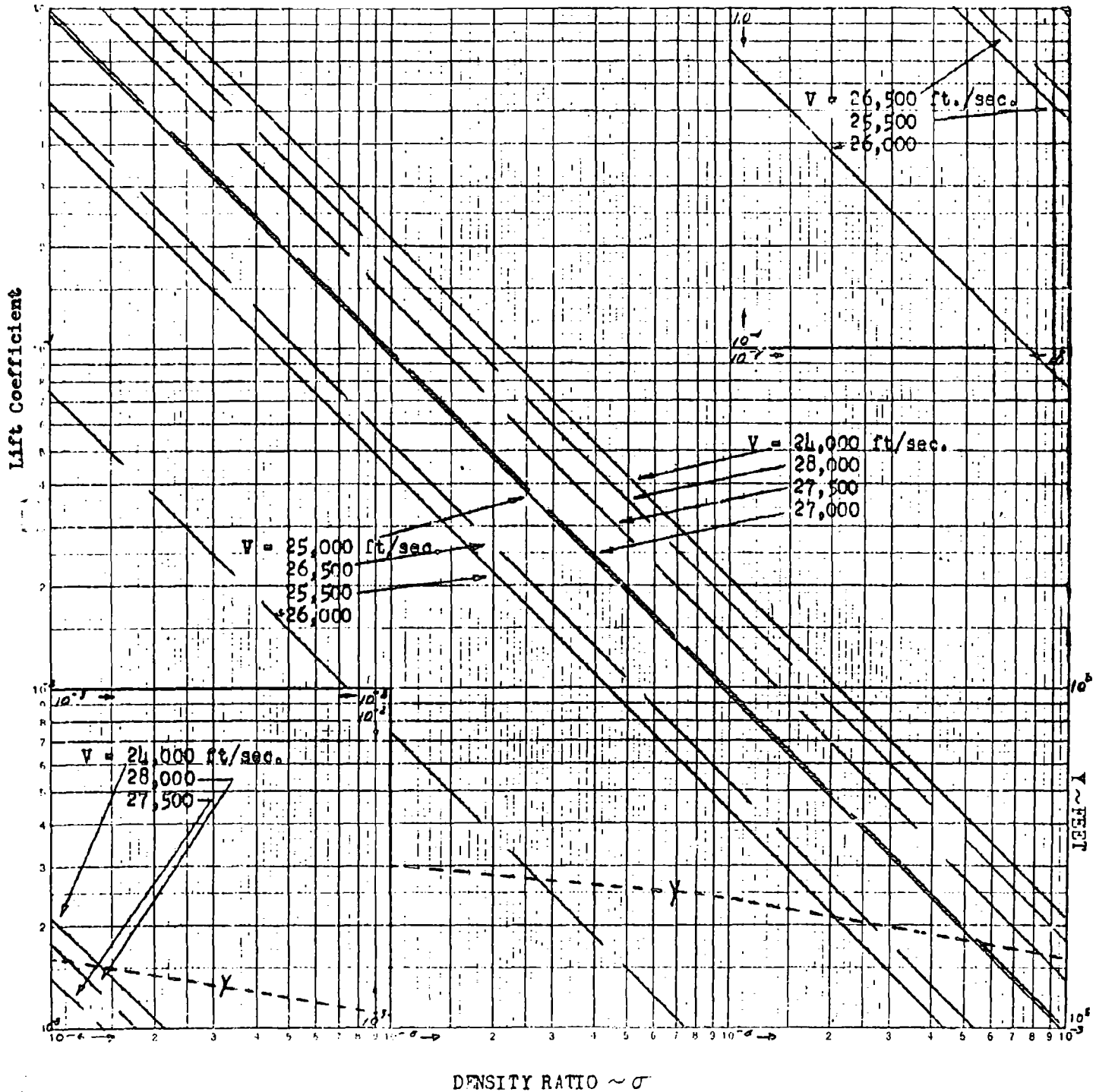
DENSITY RATIO $\sim \sigma$

——— Velocities < circular velocities
— — Velocities > circular velocities

FIGURE 9   EQUILIBRIUM DENSITY RATIO AT VARIOUS
FLIGHT VELOCITIES AS A FUNCTION OF LIFT
COEFFICIENT FOR A WING LOADING OF 15 lb/ft

DENSITY RATIO ~ σ

——— Velocities < circular velocities
— — Velocities > circular velocities
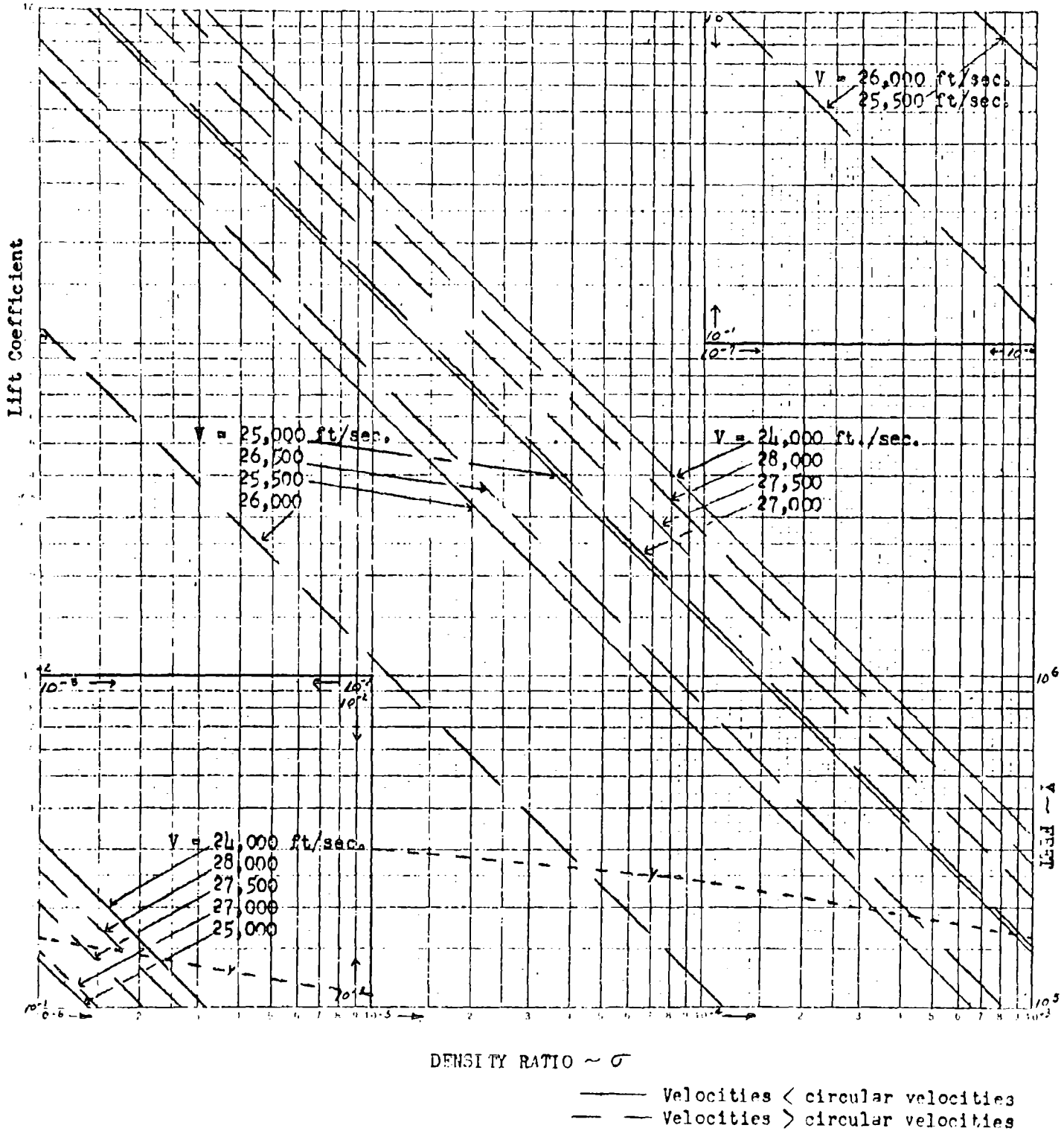
FIG. 10 - EQUILIBRIUM DENSITY RATIO AT VARIOUS
FLIGHT VELOCITIES AS A FUNCTION OF LIFT COEFFICIENT
FOR A WING LOADING OF 20 LB/FT^2

DENSITY RATIO ～ σ

Velocity < Circular Velocities
Velocities > Circular Velocities
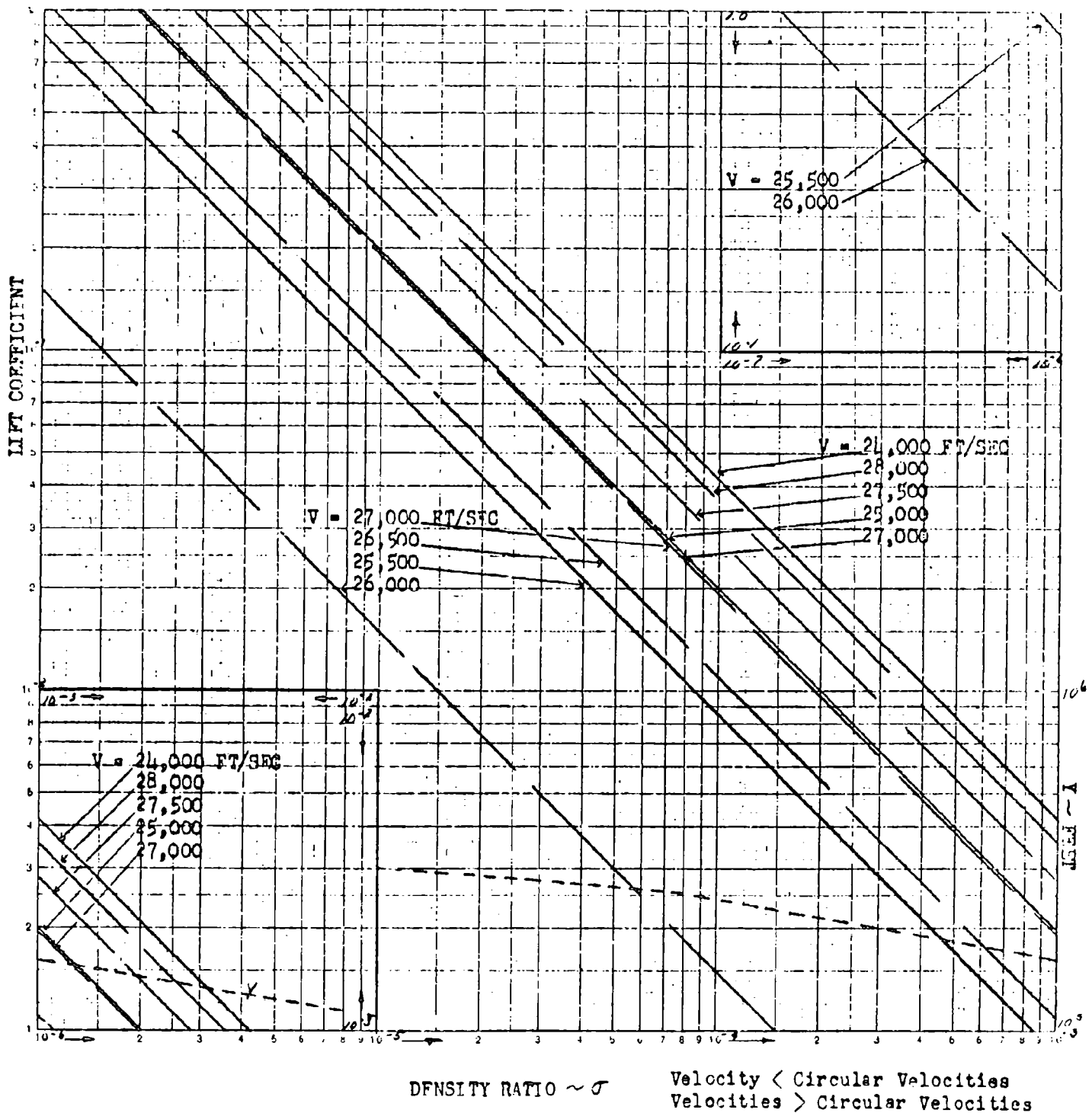
FIGURE 11 EQUILIBRIUM DENSITY RATIO AT VARIOUS
FLIGHT VELOCITIES AS A FUNCTION OF LIFT
COEFFICIENT FOR A WING LOADING OF 25 lb/ft^2
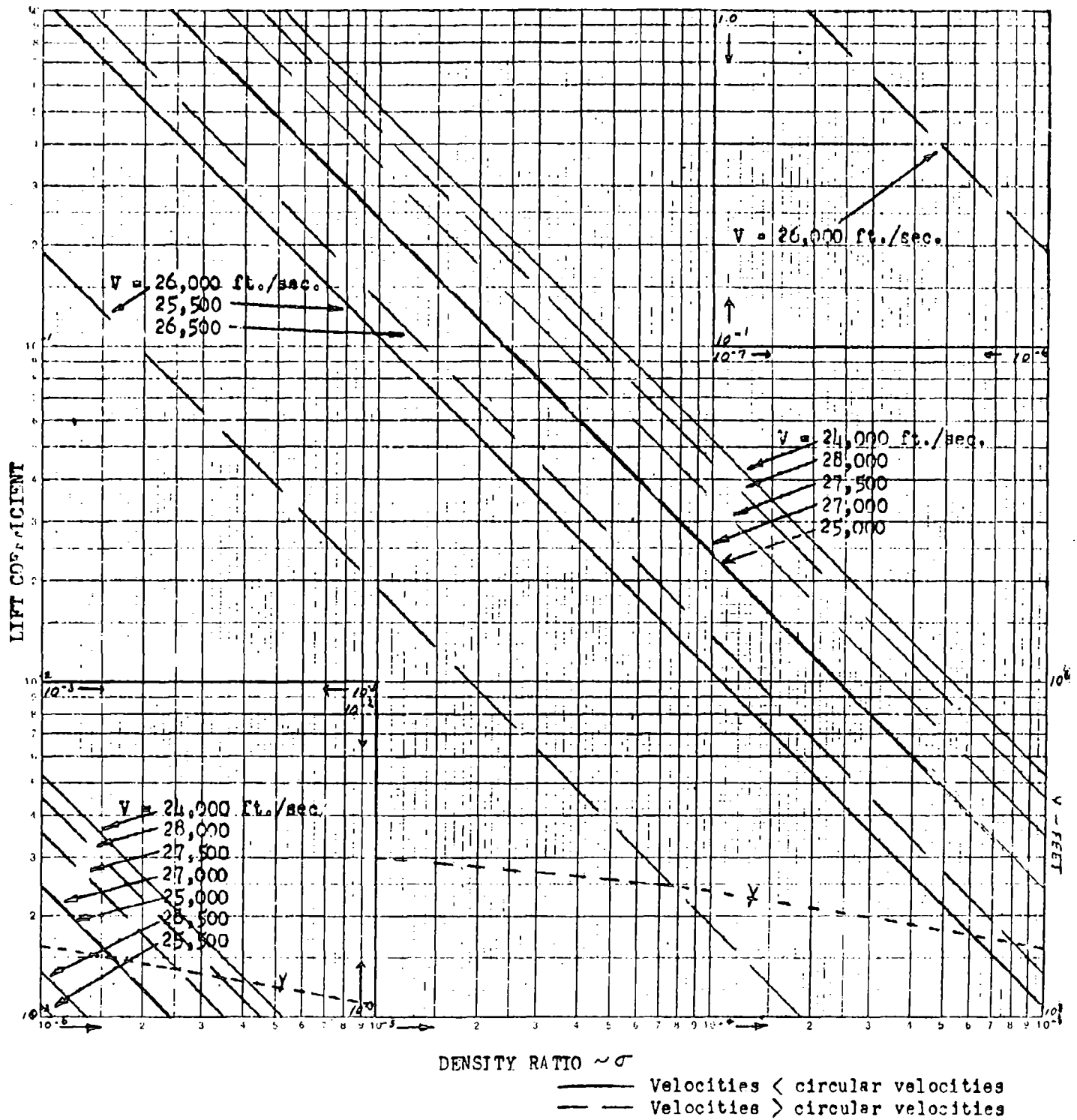
FIGURE 12   GLIDE RANGE VS. INITIAL VELOCITY

By ——————— Date ———————
Checked ——————— Date ———————
B E L L Aircraft CORPORATION
Model ——————— Page 23
Missile
Airplane ——————— Report D143-945-014

flight. The earth's circumference is 21,600 nautical miles, hence, with a range, obtained during powered ascent, of the order of 700 nautical miles, a full circumnavigation can almost be obtained after the vehicle speed is decreased to 25,000 feet per second.

Prior to this, its motion will be comparable to that of a non-winged vehicle, as pointed out before. For such a vehicle a path calculation has been presented (Reference 5), beginning at an altitude of 528,000 feet (100 miles). By the time the vehicle has descended to about 300,000 feet its velocity is approximately 25,000 feet per second and it has covered a range of 13,200 miles (11,500 nautical miles). This is more than one half circumnavigation, and shows that this altitude probably is too high for one circumnavigation of a winged vehicle. A rough estimate shows that, beginning at 400,000 feet altitude with circular velocity, a range of about 4000 nautical miles is covered until the beginning of aerodynamic flight.

These preliminary results indicate that an initial altitude of 400,000 to 450,000 feet and circular velocity as initial speed will enable the vehicle to complete one circumnavigation and to operate during the aerodynamic portion of the flight at maximum lift rather than maximum lift-over-drag ratio. For more than one revolution, however, the initial altitude, according to the results of Reference 5, will have to be greater than 500,000 feet and of the order of 600,000 feet.

The computation of trajectories for powered ascent into such a path shows that, for three stages and initial accelerations of the order of 1.3g for the first stage, a ratio of actually attained velocity to ideal velocity which could be obtained in the absence of gravity and drag of

$$\frac{\Delta v_{tot}}{(\Delta v)_{id}} \simeq 0.85 \text{ to } 0.89.$$

For $\Delta v_{tot} = 25,800$ feet per second, the resulting ideal velocity for which the mass ratio of the complete vehicle must be designed is therefore of the order of 29,000 to 30,000 feet per second.

VI. PATH TYPE II: ELLIPTIC

The elliptic path offers the possibility for placing a considerable portion of the flight path into vacuo, thereby minimizing the duration of action of dissipative forces on the vehicle during each revolution. The action of these forces is confined to the section of the flight path near the perigee.

On the other hand, the elliptic path involves motion at varying speed and altitudes above the surface. The greatest altitude and the lowest speed are attained at the apogee. Lowest altitude and highest speed occur at the perigee. For the low-eccentricity ellipses under consideration here, the difference in speed will be comparatively less important than the difference in altitude, because relatively minor velocity variations at the perigee (of the order of a few hundred feet per second) involve changes in altitude which are significant from the viewpoint of radar reconnaissance and bombing. If the elliptic path section over the target area lies between the before-mentioned apsides, then the vehicle experiences the greatest rate of change of altitude as well as of speed when this is least desirable from the viewpoint of mission effectiveness. For this reason the perigee should be located over the target area (the altitude variations are small for a considerable distance before and after passing the perigee point).

The simplest and least expensive powered ascent is the ascent directly into the perigee of a given elliptic orbit. However, the perigee would then be located near the launching site, that is, over friendly territory. This is undesirable for the reasons previously given.

Therefore, it is necessary to launch the vehicle at an inclination corresponding to a point on the ellipse preceding the apogee. The arrangement must be such that the apogee is reached at the opposite side of the earth from the target area. It can be shown that for ellipses whose apogees are relatively close to the launching site and which, at the same time, are at a relatively low altitude, it is not possible to place the perigee at an adequate altitude above the target area. In fact, the theoretical perigee point lies in these cases inside the earth. Therefore, it is necessary to change the ellipse by a moderate impulse (short burst of power). It is assumed that this impulse is applied exactly at the apogee. For the sake of simplicity, it is also assumed that the impulse is applied instantaneously, that is exactly at the apogee point, rather than over a certain path length around the apogee. This

assumption involves a small or negligible error even if, for reasons of accuracy, a very small thrust (acceleration) is applied, because the required velocity increments are small, as will be seen from the following material.

Referring to Figure 1 in Reference 4, taking Sverdlovsk as center of the target area, it follows that the apogee must be located at a surface distance of approximately 4,000 to 5,000 nautical miles from the take-off point in the direction opposite to the shortest great circle direction from the take-off point to the center of the target area.

This criterion fixes the approximate distance of the apogee. The altitude may vary within certain limits which are derived from the following considerations:

1. The apogee must be high enough to eliminate dissipative air forces over a major portion of the path. This is one of the principal advantages of the elliptic path and permits repeated revolutions at little additional energy.

2. The apogee should not be too high, because the over-all energy requirement increases with the apogee distance. Therefore, going to an unnecessarily high apogee, will ultimately cancel the effect of the absence of dissipative forces on the over-all energy requirement. Moreover high apogee distance leads to high perigee velocity, imposes increased accuracy requirements for the apogee impulse, and leads to a considerable variation of flight altitude along the path. This last effect may not be desirable from the viewpoint of auxiliary radar navigation.

Consequently, the apogee altitude should not be greater than necessary for compliance with the first requirement. This requirement will limit the minimum apogee altitude to a value of the order of 150 nautical miles (about 900,000 feet). The simultaneous requirement of a horizontal apogee distance of 4000-5000 nautical miles imposes a near-circular cut-off velocity on the flight program.

Based on known relations from the mechanics of elliptic flight paths, a number of elliptic paths have been calculated and condensed in a set of graphs (Figures 13 through 19). The relations which have been derived in a form convenient for the present purpose in Reference 6 are numerical eccentricity

FIGURE 13 ELLIPTIC PATH SURFACE DISTANCE BETWEEN CUT-OFF POINT AND APOGEE AS FUNCTION OF ANGLE OF DEPARTURE FOR DIFFERENT V_1/V_e

$\frac{V_1}{V_s}$

1.0

0.994

0.975

0.95

DISTANCE BETWEEN CUT-OFF POI. AND APOGEE ~ 1000 NAUT. MI.

TRAJECTORY ANGLE AT CUT-OFF (θ_1) - DEGREES

FIGURE 14 ELLIPTIC PATH-SURFACE DISTANCE BETWEEN CUT-OFF POINT AND APOGEE AS FUNCTION OF V_1/V_C FOR DIFFERENT ANGLES OF DEPARTURE.

DISTANCE BETWEEN CUT-OFF POINT AND APOGEE ~ 1000 N. MI.

CUT-OFF VELOCITY/CIRCULAR VELOCITY
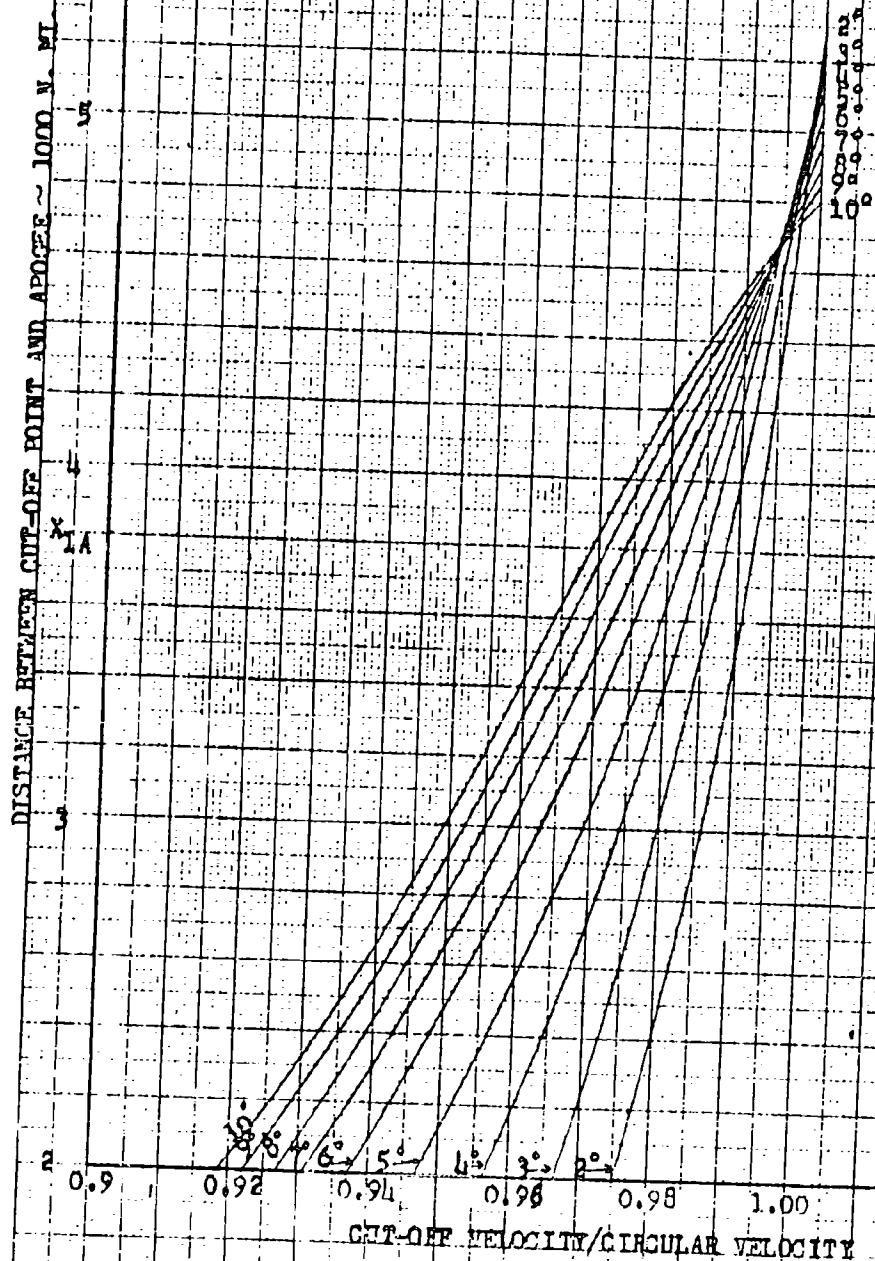
FIGURE 15 - ELLIPTIC PATH - SUMMIT ALTITUDE AS FUNCTION OF ANGLE OF DEPARTURE FOR DIFFERENT CUT-OFF VELOCITIES

SUMMIT ALTITUDE ~ 10^6 FT.

TRAJECTORY ANGLE AT CUT OFF - θ, ~ DEGREES

SECRET

FIGURE 16. ELLIPTIC PATH - SUMMIT ALTITUDE AS FUNCTION OF CUT-OFF VELOCITY FOR DIFFERENT ANGLES OF DEPARTURE.

CUT-OFF VELOCITY/CIRCULAR VELOCITY
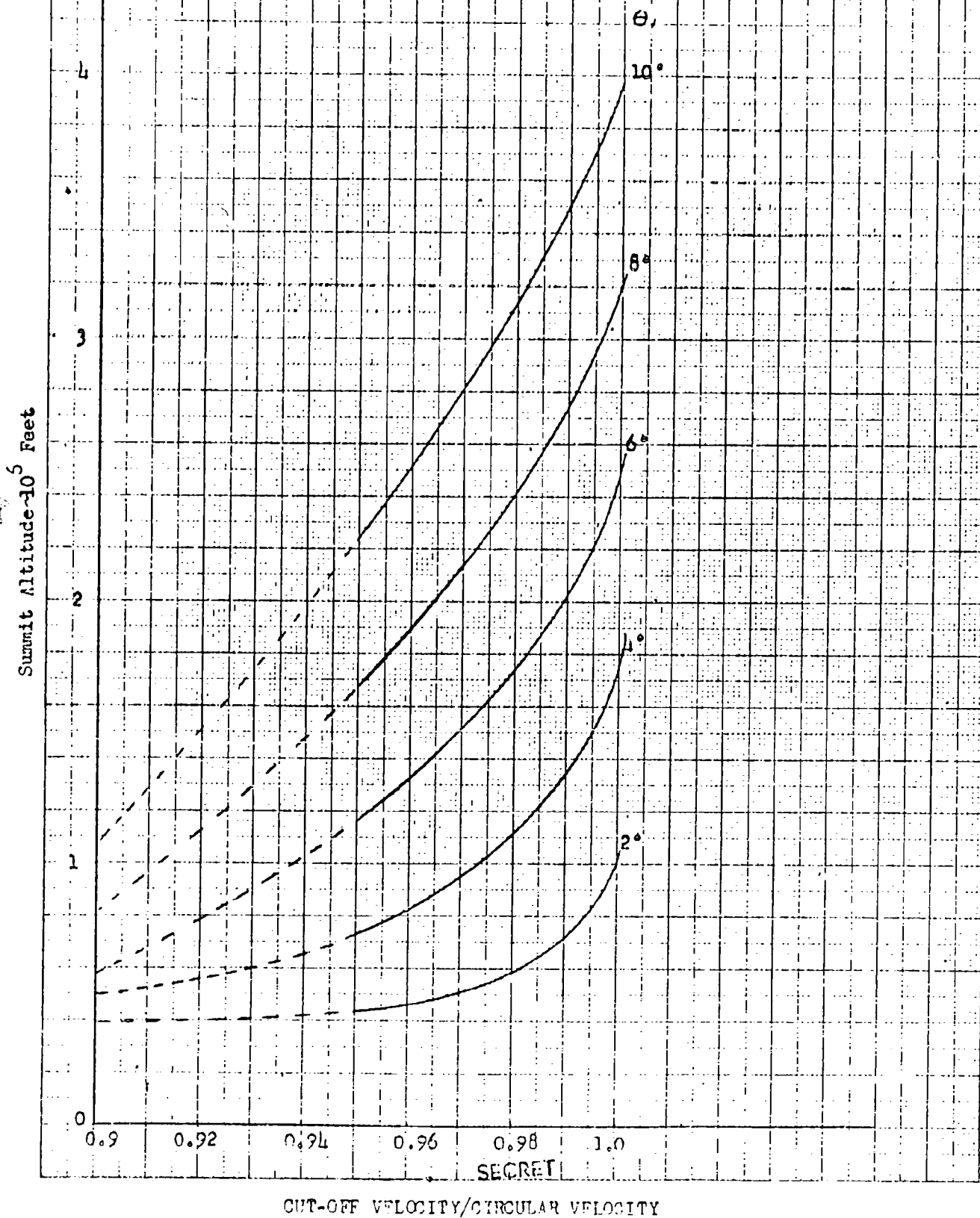
FIGURE 17 - ELLIPTIC PATH - APOGEE VELOCITY INCREMENT REQUIRED AS FUNCTION OF CUT-OFF VELOCITY

θ, TRAJECTORY ANGLE AT CUT-OFF~DEGREES

SECRET
BELL Aircraft Corporation

BY_____DATE_____
CHECKED_____DATE_____
MODEL_____PAGE___31___
SHIP_____REPORT D143-945-014

FIGURE 1B ELLIPTIC PATH - APOGEE VELOCITY INCREMENT REQUIRED AS FUNCTION OF CUT-OFF VELOCITY

VELOCITY INCREMENT ~ FT/SEC.
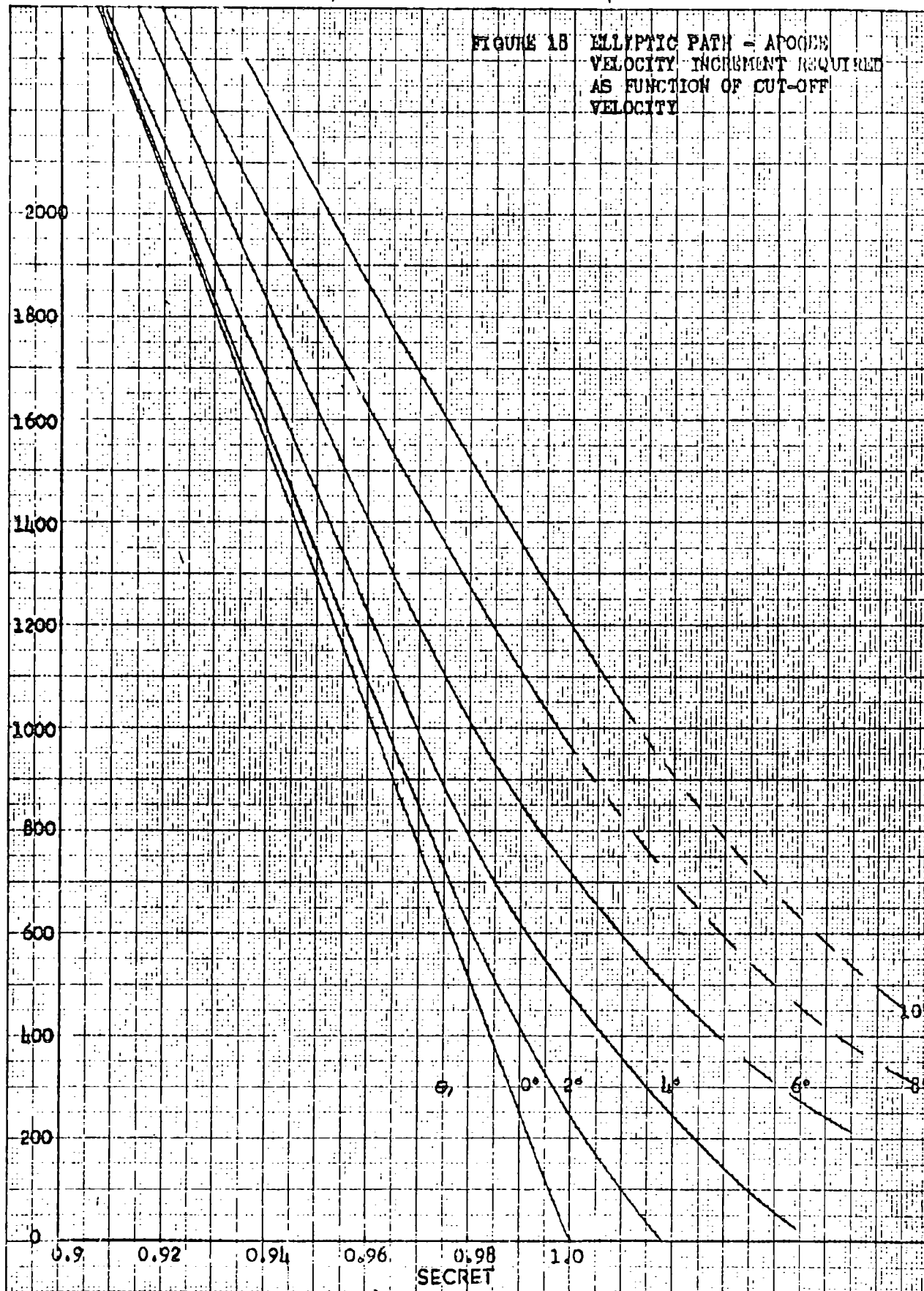
CUT-OFF VELOCITY / CIRCULAR VELOCITY

FIGURE 19 ELLIPTIC PATH - FLIGHT TIMES ALONG DIFFERENT SECTIONS
AS FUNCTION OF ANGLE OF DEPARTURE

FLIGHT TIME ~ MINUTES

$\Delta t_{r_1 P}$ (FLIGHT TIME BETWEEN CUT-OFF AND PERIGEE)

$V_1/V_c = 1.0$

0.975

0.95

1.0

$\frac{T'}{2}$ (HALF PERIOD OF MODIFIED ELLIPSE) 0.975 0.95

$\Delta t_{r_1 A}$ (FLIGHT TIME BETWEEN CUT-OFF AND APOGEE
1.0

0.975

0.95

SECRET

TRAJECTORY ANGLE AT CUT-OFF ~ θ, DEGREES

SECRET

By _____ Date _____   BELL Aircraft CORPORATION   Model _____ Page 33
Checked _____ Date _____   Missile / Airplane _____ Report D143-945-014

$$e = \sqrt{(1 - q_1)^2 + q_1^2 \tan^2 \theta_1} \quad \text{-------------} \quad (5)$$

$$q_1 = \left(\frac{v_1}{v_c}\right)^2 \cos^2 \theta_1 \quad \text{----------------} \quad (6)$$

(θ_1 = trajectory angle at cut-off = angle of departure)

$$v_1 = \frac{v_1}{(v_c)_1} (v_c)_1 \quad \text{-------------------} \quad (7)$$

where the local circular velocity

$$(v_c)_1 = \sqrt{\frac{\gamma}{r_1}} \quad \text{------------------} \quad (8)$$

and $\quad \gamma = 1.4055 \times 10^{16} \text{ ft}^3/\text{sec}^2 \quad \text{--------------} \quad (9)$

The cut-off altitude y_1 has been taken as 300,000 feet in all numerical cases below. The apogee distance is

$$r_A = r_1 \frac{q_1}{1-e} \quad \text{---------------------} \quad (10)$$

velocity at the apogee

$$v_A = v_1 \cos \theta_1 \frac{r_1}{r_A} = (v_c)_1 \sqrt{q_1} \frac{r_1}{r_A} \quad \text{---------} \quad (11)$$

Semi-major axis

$$a = \frac{r_A}{1 + e} \quad \text{-----------------------} \quad (12)$$

Form K4-1 Rev. 353

perigee distance

$$r_P = a(1 - e) \ \text{-----------------------} \ (13)$$

half center angle of path (δ = true anomaly η minus 180°)

$$\tan \delta_1 \quad = \frac{q_1 \tan \theta_1}{1 - q_1} \left(= \frac{1}{\tan \theta_1} \ \text{if} \ \frac{v_1}{v_c} = 1.0 \right) \ \text{-----} \ (14)$$

range on surface from cut-off point to summit point (apogee)

$$X_{1A} = r \ \delta^{(r)} \ \text{----------------------} \ (15)$$

Since $r_P < r_{oo}$, the ellipse is modified at the apogee by means of an impulse, in order to obtain a suitable new perigee distance over the target area. This distance has been taken in all calculations as 2.119×10^7 feet ($y_A = 300,000$ feet). Designating all values pertaining to the modified ellipse by a prime, one obtains

$$\frac{v'_A}{(v_c)_A} = \sqrt{\frac{2 r'_p}{r_A + r'_P}} \ \text{------------------} \ (16)$$

The new apogee velocity is therefore

$$v'_A = \frac{v'_A}{(v_c)_A} \quad (v_c)_A \ \text{------------------} \ (17)$$

yielding the velocity increment required at the apogee

$$\Delta v_A = v'_A - v_A \ \text{--------------------} \ (18)$$

The characteristic values of the modified ellipse are

$$a' = \frac{r_A + r_P}{2} \ \text{----------------------} \ (19)$$

By _____ Date _____

Checked _____ Date _____

BELL *Aircraft* CORPORATION

Model _____ Page __35__

Missile
Airplane _____ Report D143-945-014

parameter

$$p' = q_A r_A = \left[\frac{v'_A}{(v_c)_A} \right]^2 r_A \quad \text{- - - - - - - - - - - - -} \quad (20)$$

$$e' = \sqrt{1 - \frac{p'}{a'}}$$

$$v'_p = v_A \frac{r_A}{r'_p} \quad \text{- - - - - - - - - - - - - - - - - - - -} \quad (22)$$

Aside from using the Kepler equation, the flight time between two points on an elliptic path can also be found from Kepler's second law, counting the time from the perigee and using the true anomaly η

($\eta = 0$ at the perigee), by integrating the equation

$$dt = \frac{r^2}{C} d\eta \quad \text{- - - - - - - - - - - - - - - - -} \quad (23)$$

where C is the constant of Kepler's area law. Integrating this equation (Reference 6)

$$\Delta t = \frac{1}{C} \int_{\eta_1}^{\eta_2} r^2 d\eta \quad \text{- - - - - - - - - - - - - - - - - - - -} \quad (24)$$

eliminating C by means of the relation

$$\frac{p^2}{C} = \sqrt{\frac{p^3}{\gamma}} \quad \text{- - - - - - - - - - - - - - - - - - -} \quad (25)$$

and expressing the result in terms of numerical eccentricity and radial distance, yields for the flight time between two points, 1 and 2, on the ellipse (counting always from perigee to apogee in either direction to avoid true anomalies $\eta > 180°$)

Form E4-1 Rev. 353

$$\Delta t = \frac{\sqrt{\frac{p}{\gamma}}}{1-e^2}\left[\sqrt{2pr_1 - r_1^2(1-e^2)-p^2} - \sqrt{2pr_2 - r_2^2(1-e^2)-p^2}\right.$$

$$\left. +\sqrt{\frac{p}{1-e^2}}\left[\sin^{-1}\left(\frac{r_2(1-e^2)-p}{ep}\right) - \sin^{-1}\left(\frac{r_1(1-e^2)-p}{ep}\right)\right]\right] (26)$$

For calculating the time between a cut-off distance r_1 and apogee ($\eta_2 = 180°$), the second square root term in Equation (26) becomes zero. Figures 13 and 14 show the surface range X_{1A} covered between cut-off point and summit point as function of the cut-off angle θ_1 (angle of departure) for different ratios v_1/v_c and as function of v_1/v_c for different values of θ_1. It is interesting to note that for a v_1/v_c around 0.994 the angle of departure has practically no effect on X_{1A}. The reason for this is that, as Figure 13 indicates, there is a certain θ_1 for maximum X_{1A} for each v_1/v_c. This optimum angle for maximum range decreases with increasing v_1/v_c and is zero for $v_1/v_c = 1$. Therefore, for all $v_1/v_c < 1$, X_{1A} first increases with θ_1, reaches a maximum, and then decreases again. For $v_1/v_c = 1$, however, X_{1A} decreases monotonically with $\theta_1 > 0°$. Therefore, plotting X_{1A} versus v_1/v_c must yield a cross-over point of curves of different θ_1. It is seen that for angles of departure $\theta_1 \leqq 10°$ it is necessary that $v_1/v_c \geqq$ 0.975, if $X_{1A} \geqq$ 4000 nautical miles.

Figures 15 and 16 show the variation of the apogee (or summit) altitude as function of angle of departure and v_1/v_c, respectively. The altitudes shown are considerable and indicate that it is important to keep the angle of departure as small as possible within the limits of the other requirements.

The velocity increment required to modify the ellipse by an impulse at the apogee is shown in Figures 17 and 18 as a function of angle of departure and v_1/v_c. As was to be expected, the energy requirement decreases rapidly with decreasing angle of departure. For large values of v_1/v_c and small values of θ_1, the required velocity increment is very small and should not affect unduly the design of the upper stage.

Three sets of curves designating the flight time along different sections of the elliptic path are presented in Figure 19, where $\Delta T_{r_1 A}$ designates the flight time between cut-off and apogee, $\frac{T^1}{2}$ is the half-period of the modified ellipse, after the apogee impulse has been applied, and $\Delta T_{r_1 P}$ represents the flight time from cut-off to the perigee, that is to the target area. The flight time for the residual portion of the path between target area and launching site depends on whether another revolution is planned, or whether the vehicle descends to the surface. In any case the approximate flight time for this portion is of the same order of magnitude as $\Delta T_{r_1 A}$. Figure 19 shows that a vehicle, following any of the elliptic paths indicated, will coast about one hour to cover the distance from cut-off point to target area.

During the coasting period, conditions of weightlessness exist in the vehicle. Not until the vehicle approaches the perigee will an increasing amount of force due to deceleration be felt, due to the growing dynamic pressure. Figure 20 shows this dynamic pressure for local circular velocity as function of flight altitude. It also shows the deceleration in surface g's for a lifting area load of 20 pounds per square foot and a drag coefficient of 0.7, based on diffuse reflection of the molecules from the wall in free-molecule flow.(Reference 3). This drag coefficient is probably conservative for altitudes below 300,000 feet where a boundary layer begins to form. According to Figure 20, the deceleration at the perigee reaches a maximum of 0.2 to 0.3g. (The vehicle velocity at the perigee is not much greater than local circular velocity as is shown later in this section.) It can also be seen that above 500,000 feet the deceleration due to drag becomes negligible.

The over-all energy requirement for the elliptic paths, expressed as ideal velocity, is plotted in Figure 21 as a function of the angle of departure for three values of $v_1/v_c = 0.95, 0.975,$ and 1.0. The ideal velocity in each instance if found by assuming a velocity factor $\Delta v_{tot} / \Delta v_{id}$ (cf. Section IV) for the powered ascent and by adding to the resulting value the velocity increment produced at the apogee. For this increment it is possible, with good accuracy, to take the velocity factor as being one, because propulsion occurs in vacuo and practically in a direction normal to the radius vector. An upper and a lower limit have been given for values of Δv_{id}, the upper limit resulting from taking $\Delta v_{tot} / \Delta v_{id} = 0.85$, the lower limit by taking

FIGURE 20 DYNAMIC PRESSURE AND DECELERATION AT
CIRCULAR VELOCITY AS FUNCTIONS OF ALTITUDE.

$C_{Dq} \frac{S}{W}$

$C_D = 0.7$

$\frac{S}{W} = 20 \text{ LB/FT}^2$

$V = \sqrt{\frac{r}{r}} = \text{local } V_c$

$C_{Dq} \frac{S}{W} (g_\infty)$

q

$[16/\text{FT}^2]$

ALTITUDE ~ 1000 FT.
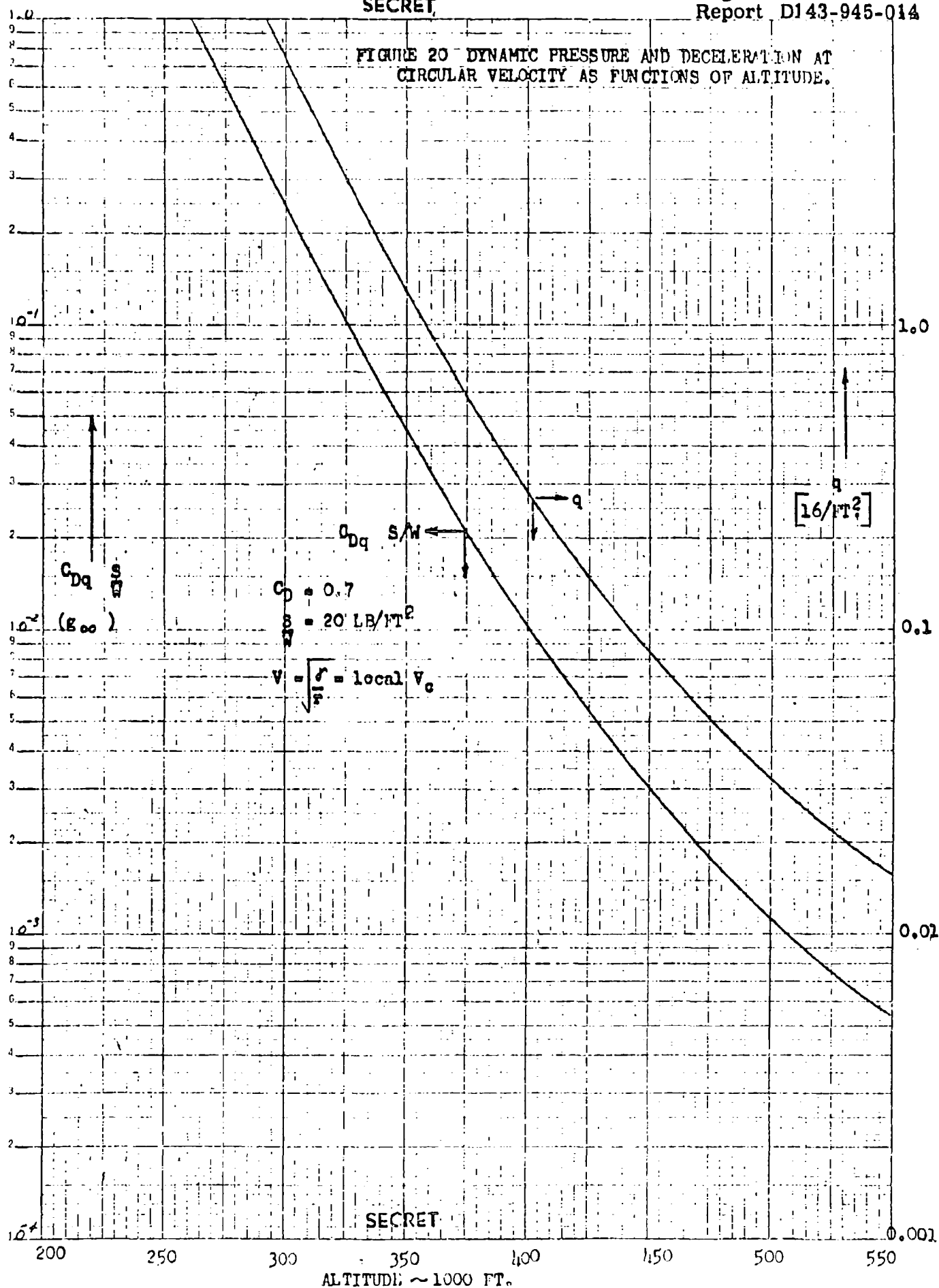
FIGURE 21 ELLIPTIC PATH - IDEAL VELOCITY
REQUIREMENT FOR DIFFERENT INITIAL
VELOCITIES AS FUNCTION OF ANGLES
OF DEPARTURE.

Upper Limit: $\dfrac{\Delta V_{tot}}{\Delta V_{id}} < 0.85$

Lower Limit: $\dfrac{V_{tot}}{V_{id}} = 0.89$
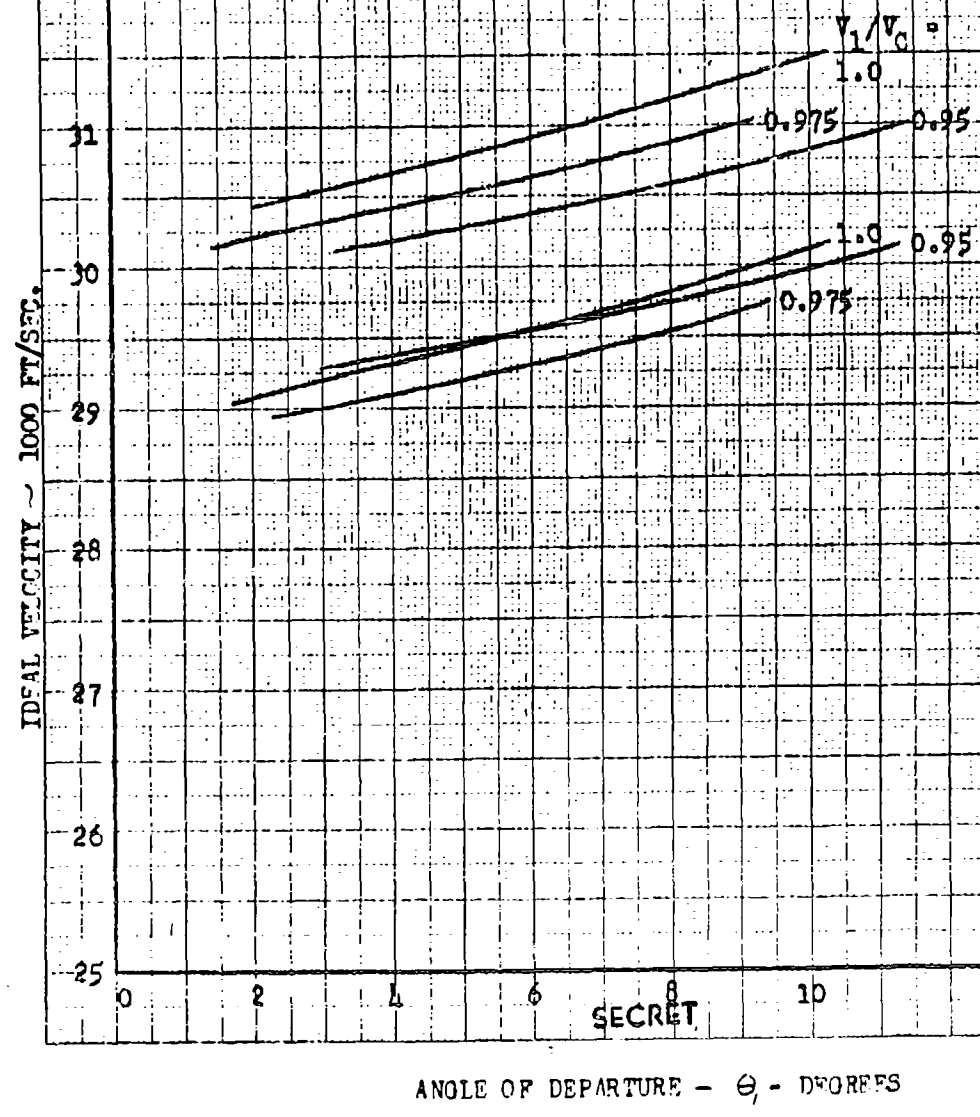
$V_1/V_c =$

1.0

0.975   0.95

1.0   0.95

0.975

IDEAL VELOCITY ~ 1000 FT/SEC.

ANGLE OF DEPARTURE - Θ_1 - DEGREES

SECRET

this factor as 0.89, Δv_{tot} being identical with $(v_1/v_c)v_c$. It can be seen that for small angles of departure (2 to 4 degrees) and $0.975 \leq v_1/v_c \leq 1.0$, the ideal velocity is of the order of 29,000 to 30,500 feet per second, that is, about the same as for the spiral path. It is indicated, however, that the use of larger angles of departure rapidly increases the ideal velocity to values between 30,000 and 31,500 feet per second.

The application of a small angle of departure is therefore desirable for several reasons:

1. In order to avoid unnecessarily large apogee distances.

2. In order to keep the energy requirement at the apogee, for modification of the elliptic path, as small as possible.

3. In order to keep the over-all energy requirement for the elliptic path small.

Since, at the same time, the requirement of an apogee location is 4000 to 5000 nautical miles from the take-off point must be satisfied, the desirability of a small angle of departure automatically leads to cut-off velocities of v_1/v_c of 0.98 to 0.995.

From the viewpoint of flight accuracy, these results have the following significance. Figure 14 shows a cut-off velocity of v_1/v_c of 0.995 to be desirable because errors in the angle of departure in this velocity range are seen to be of very small importance for the accuracy of the horizontal apogee distance, hence also for the horizontal distance of the perigee and, therefore, for the appearance over the target area at correct altitude.

However, Figure 16 shows that with increasing v_1/v_c this apogee altitude becomes increasingly sensitive to errors in cut-off velocity at a given angle of departure. However, Figure 16 as well as Figure 15 indicate some alleviation of accuracy requirements with decreasing angle of departure.

By the same token, a small angle of departure at near-circular velocity also reduces the sensitivity of the perigee distance to errors during the apogee propulsion period *. This is particularly important

* It can be assumed that errors at cut-off will be corrected by the apogee impulse. In this case only errors at the apogee will affect errors at the perigee.

in view of Figure 20, which shows that a relatively small error in apogee distance, especially to the lower side, can become very dangerous to vehicle and pilot. A perigee altitude of 250,000 feet instead of 300,00 · feet will increase deceleration many times (about 5 times according to Figure 20) and will change the aerodynamic heating conditions correspondingly. Such an error, however, corresponds to an error of only 2.114/2.119 = 0.99764 or 0.236 percent in perigee distance r_p, based on an earth radius of $r_{oo} = 2.085 \times 10^7$ feet. In this critical perigee-distance-accuracy-requirement lies the greatest penalty to be accepted for the otherwise favorable characteristics of the elliptic path.

In order to find the energy requirement for additional revolutions, it is necessary first to estimate the drag losses encountered in the perigee region.

From the polar equation of a conic

$$r = \frac{p}{1 + 2 \cos \eta} \quad\text---------------- \quad (27)$$

which, by definition as to the counting of the true anomaly η from the perigee, becomes for the perigee distance

$$r_p = \frac{p}{1 + e} \quad\text---------------- \quad (28)$$

From this one obtains

$$\frac{r_p}{r} = \frac{1 + e \cos \eta}{1 + e} \quad\text---------------- \quad (29)$$

or

$$\cos \eta = \frac{\frac{r_p}{r} (1 + e) - 1}{e} \quad\text---------------- \quad (30)$$

For the eccentricities of the modified ellipses values between 0.02 and 0.06 are found. Assuming e = 0.04 and the altitude where drag becomes significant as y = 500,000 feet so that r = 2.139 x 10^7 feet, there is obtained with r_p = 2.119 x 10^7 feet (y_p = 300,000 feet)

$$\cos \eta \cong \frac{1.02 - 1}{0.03} = 0.6667$$

$$\eta \cong 48.2° = 0.8407^r$$

The horizontal distance covered between the 500,000-foot and the 300,000-foot level is then approximately

$$s = \frac{r + r_p}{2} \times 0.8407 = 1.79 \times 10^7 \text{ feet} = 2944 \text{ nautical miles.}$$

In other words, deceleration acts in this case as a rather low eccentricity ellipse over a distance of $2S \approx 6000$ nautical miles. The deceleration is given by $D/m = q g C_D S/W$ so that

$$\frac{dv}{dt} = - \frac{q g C_D S}{W} \quad \text{- - - - - - - - - - - - - - - - - - -} \quad (31)$$

Using the relation

$$\frac{ds}{dt} = v \quad \text{- -} \quad (32)$$

one can write

$$\frac{dv}{ds} = \frac{dv}{dt} \times \frac{dt}{ds} = - q g C_D \frac{S}{W} \frac{1}{v}$$

which can be transformed into the differential equation

$$\frac{dv}{v} = - \frac{\rho}{2} g C_D \frac{S}{W} ds \quad \text{- - - - - - - - - - - - - - -} \quad (33)$$

By _____ Date _____
Checked _____ Date _____

B E L L *Aircraft* CORPORATION

Model _____
Missile
Airplane _____

Page ___43___
Report __D143-945-014__

which, upon integrating with v_i as "inertial" velocity (i.e., velocity when crossing the 500,000-foot level) yields

$$\ln \frac{v}{v_i} = \frac{\rho_0}{2} g \, C_D \frac{S}{W} s = - \frac{\sigma g}{841} \frac{C_D s}{W/S} \quad\text{----- (34)}$$

where s is the length of path, counting from the point on where the 500,000-foot level is intersected, and $\rho_{oo}/2 = \frac{1}{841}$. Taking for s the whole path length from the intersection of the 500,000-foot level to the perigee, the value has been found before to be s $\sim$ 1.8 x 10^7 feet, and assuming W/S = 20, C_D = 0.7, and σ = 3.6 x 10^{-7} (corresponding to about 400,000 feet altitude) one obtains $\ln \frac{v}{v_i} \approx$ - 0.0083

$$v = 0.9917 \times v_i \quad\text{--------------------- (35)}$$

Less than one percent of the speed at 500,000 feet is lost when the vehicle arrives at the perigee. It may be emphasized that this result has been obtained in spite of rather conservative assumptions; namely, a small eccentricity, which results in a large path length s, and a large drag coefficient.

Figure 22 shows the theoretical velocity v_p' at the perigee of the modified ellipse in the range 0.95 $\le$ v_1/v_c $\le$ 1.0 as a function of the angles of departure. The value of the elliptic excess v_p' - $(v_c)_{300,000}$ is seen to range between 120 and 1000 feet per second in the extreme cases or between about 200 and 600 feet per second for v_1/v_c close to unity and small angles of departure. One per cent velocity loss amounts to about 260 feet per second. This means that the vehicle, when arriving at the perigee has nearly local circular velocity. Taking the losses between perigee and the point of crossing the 500,000-foot level on the way out, into account, the total velocity loss will amount to 400 to 600 feet per second, and this is the velocity increment required at the perigee to send the vehicle off to a second circumnavigation. In view of the conservative assumptions made, the actual value may well lie somewhere between 1/2 and 3/4 of this number, that is, be of the order of 300 to 400 feet per second only. Thus, energetically, the elliptic path looks very attractive if more than one revolution is desired.

This is, of course, only part of the picture. As mentioned here, the elliptic path requires great accuracy with respect to scalar

BY_____ DATE_____ **BELL** *Aircraft* CORPORATION | MODEL_____ PAGE **44**
CHECKED_____ DATE_____ | SHIP_____ REPORT **D143-945-014**

SECRET

FIGURE 22   ELLIPTIC PATH - PERIGEE VELOCITY AS FUNCTION
OF ANGLE OF DEPARTURE

$\frac{V_1}{V_c} = 1.0$

$\frac{V_1}{V_c} = 0.95$

(V_c) 300,000 ft.

VELOCITY AT PERIGEE ~ 1000 FEET
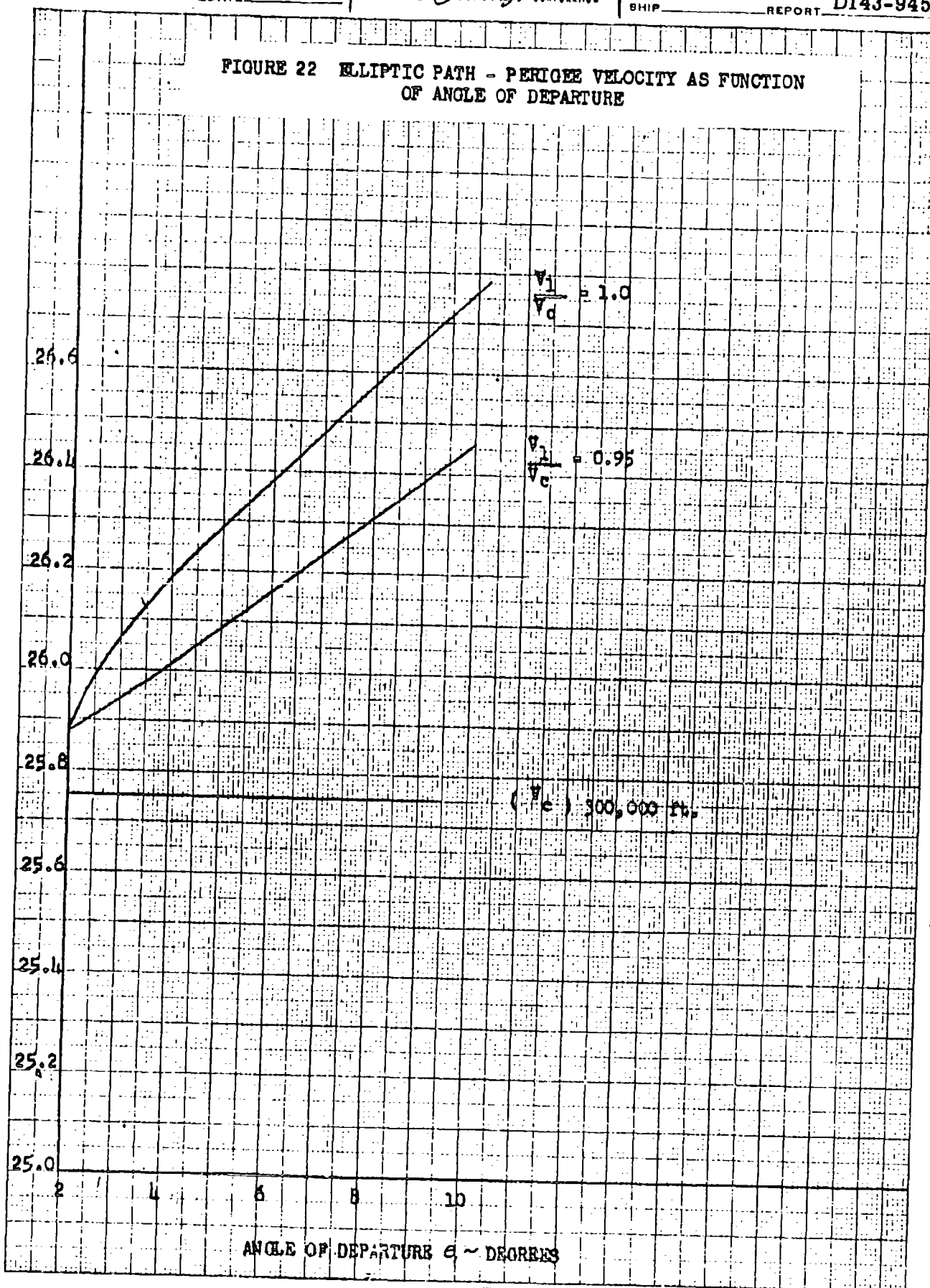
26.6

26.4

26.2

26.0

25.8

25.6

25.4

25.2

25.0

2   4   6   8   10

ANGLE OF DEPARTURE θ ~ DEGREES

magnitude and the orientation in space of the velocity vector at the end of each propulsion period. Two propulsion periods are required for the first circumnavigation, plus one more for each subsequent revolution. The energy requirement for this additional propulsion period is likewise rather sensitive for inaccuracies in the perigee distance, especially to the lower side of r_p, a condition due to the rapidly increasing air density below 300,000 feet. For instance, if y_p = 250,000 feet instead of 300,000 feet, a rough estimate made using Equation (34) with the same numerical values except for σ, which is taken as 7.2×10^{-7} for y = 375,000 feet, gives v/v_1 = 0.9835. Comparison with Equation (35) shows that this value means roughly a doubling of the velocity loss. The absolute value still is not significant and, from the energy viewpoint, a perigee altitude of 250,000 feet appears still feasible, though it is probably marginal. However, the extent to which the change occurs and the velocity loss is increased, shows again the significance of high flight path accuracy which has already been found in connection with the flight-mechanical discussion of the elliptic path without air drag.

The descent back to the surface appears to be particularly favorable in the case of the elliptic path. Arriving at the perigee, the vehicle velocity is about circular, with only 4000 to 5000 nautical miles to go between target area and take-off point. Even a maximum lift descent furnishes more than this range. The vehicle therefore can deviate from the great circle route as soon as the velocity is low enough that no severe aerodynamic heating occurs from the resulting decrease in equilibrium altitude. Sufficient power is available to approach the launching site gradually, and with a greater safety margin.

The over-all conclusion which may be formulated on the basis of the preceding results is that the elliptic path is very attractive, inasmuch as it offers the possibility for several circumnavigations, each at very little additional expense beyond what has to be spent initially for the first circumnavigation; inasmuch as this initial energy expense is not significantly larger, if it is larger at all, than that necessary for the spiral path; and inasmuch as it offers in contrast to the spiral path, the same altitude and speed over the target area, no matter what the number of circumnavigations. The elliptic path, however, requires great cut-off accuracy in order to make sure that the perigee altitude remains in the region of 250,000 to 300,000 feet. It also requires great accuracy as regards the attitude control of the vehicle when re-entering the atmosphere. And it requires an extremely well coordinated fast-responding dual control system in the

form of jet control — aerodynamic control in order to damp out posible flight path oscillation which is likely to result from inaccuracies in vehicle attitude when entering the atmosphere and from deviations from the correct perigee altitude.

The elliptic flight path, therefore, is very attractive, but apparently requires an advanced vehicle design and probably a certain amount of flight experience in the zone between space and the upper atmosphere before it can be used.

By _____ Date _____	！！ E. L. l_o/Aircraft CORPORATION	Model _____ Page ___47___
Checked _____ Date _____		Missile Airplane _____ Report D143-945-014

VII. PATH TYPE III: CONSTRAINED

The constrained circular path is a flight path flown at constant altitude and speeds ranging from above circular, to circular, or slightly less than circular. The angle of attack is varied in order to provide the required lift, beginning with a negative value, passing through zero at circular speed, and becoming positive. Not until the highest possible lift value is obtained, i.e., the lowest possible speed at the given altitude is reached, does the vehicle begin to lose altitude. Thereafter, the flight along the constrained circular path is terminated and the glide portion begins along a spiral path.

In order to fly along a constrained path, reliance on aerodynamic forces is necessary. This brings two advantages:

1. The altitude does not have to exceed 300,000 feet for the velocities in question (up to 30,000 feet per second as described later in this section). This reduces the power requirement for (hence, the weight of) airborne radar equipment, and increases the maximum feasible resolution, compared to operation at greater altitude. These factors improve — or keep at a relatively high level — the reconnaissance capabilities of the vehicle.

2. The need for aerodynamic forces means that dynamic pressure has to be present. In order to maintain a technically reasonable magnitude of aerodynamic forces, a dynamic pressure of the order of 10 pounds per square foot appears to be necessary. This dynamic pressure presumably will suffice to maintain aerodynamic control in yaw and roll also. Thus, the constrained path can be flown without control jets. Thereby, not only propellant weight is saved (which otherwise would have to be brought up to the full cutoff speed of the vehicle) but also the need for a dual control system (jet control for vacuum conditions and control surfaces for atmospheric conditions) can be eliminated. This will bring benefits in terms of weight reduction and simplification as well as reliability of the control system. However, the very presence of aerodynamic forces also implies one basic disadvantage of the constrained path. The effect of drag cuts the elliptic excess (speed above circular speed) to zero in a comparatively short time. The range covered during this period although impressive on the basis of unit time - is therefore not very large compared to the earth's circumference (20% to 50% at the most). Consequently, it appears impossible to obtain more than one revolution, and even for this the initial velocity must be considerably above circular speed, i.e., about 29,000 feet per second (circular speed 25,000 feet per

By _____ Date _____

BELL *Aircraft* CORPORATION

Model _____ Page __48__
Missile
Airplane _____ Report __D143-945-014__

Checked _____ Date _____

second). If this excess of about 3,000 feet per second is used in connection
with the spiral or elliptic path, a large number of revolutions can be made.
Another disadvantage inherent in the reliance on aerodynamic forces is
the fact that the upper surface is the lifting surface (high-pressure sur-
face) during the early flight period so that high heating occurs on the
upper surfaces at that time. Later, during the descending glide, the lower
surface is the lifting surface and the high heating occurs on this surface.
As a result, both upper and lower surfaces must be designed for high heat
fluxes, rather than just one as in the glide path.

An interesting, and perhaps significant, feature of the constrained
path is the fact that the period of weightlessness is cut down to the in-
stant when the vehicle passes the circular velocity level. At higher speed
the apparent weight is "negative" the force vector pointing upward and at
lower speed the weight is positive again.

The negative apparent weight follows from:

$$W_{app} = W (1 - \frac{v^2 r}{\gamma}) \quad - - - - - - - - - - - - - - - - \quad (36)$$

At the perigee

$$V_p^2 = \frac{\gamma}{r_p} (1 + e) \quad - - - - - - - - - - - - - - - - - - \quad (37)$$

since in the present case one can say $v = v_p$, it follows after a short
calculation

$$\frac{W_{app}}{W} \bigg|_{v > v_c} = - e \quad - - - - - - - - - - - - - - - - - \quad (38)$$

Figure 23 presents the apparent weight as a function of the flight velocity.
For inertial velocities not exceeding 29,000 feet per second, the negative
weight remains below 30 percent of the true weight and therefore is
probably not too difficult for the pilot to endure, especially since the
duration is of the order of 15 minutes or less.

SECRET
BELL *Aircraft* CORPORATION
BY_____DATE_____
CHECKED_____DATE_____
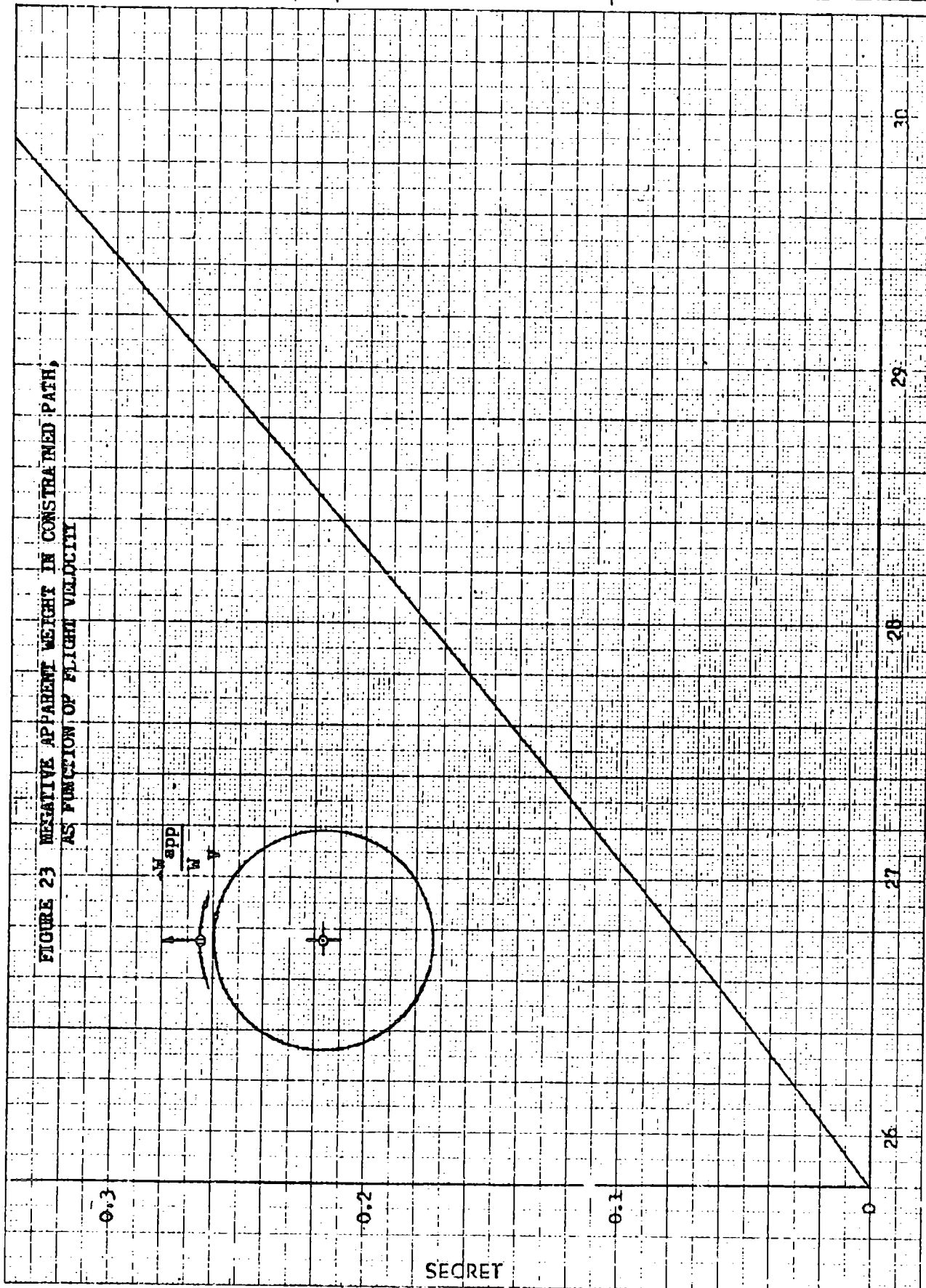MODEL_____PAGE___49
SHIP_____REPORT___D143-945-014

FIGURE 23   NEGATIVE APPARENT WEIGHT IN CONSTRAINED PATH,
AS FUNCTION OF FLIGHT VELOCITY

FLIGHT VELOCITY ~ 1000 FT./SEC.

APPARENT WEIGHT / ACTUAL WEIGHT

Figures 5 through 7 indicate that for a dynamic pressure of 10 pounds per square foot at a circular velocity of 25,800 feet per second, an altitude of 293,000 feet (56 miles or 48 nautical miles) is required.

This altitude is therefore the highest one to be taken into consideration for the constrained path, because, from the viewpoint of controllability, it permits flight at this altitude until the zero lift condition is reached. The possibility of maintaining this altitude down to a lower speed depends on the aerodynamic characteristics as well as on the lifting area load of the vehicle.

Figure 24 shows the dynamic pressure versus altitude for different flight speeds in excess of the circular velocity. The graph shows that the dynamic pressure varies less with speed than with altitude at the low densities under consideration. For instance, if the velocity is increased from 25,000 to 30,000 feet per second at the same altitude of 293,000 feet, the dynamic pressure is increased from 10 to 14 pounds per square foot.

For reasons of reducing aerodynamic heating of the vehicle, it is desirable to maintain the initial high altitude as long as possible, even at lower than circular speed (positive lift coefficient). If, on the other hand, a minimum dynamic pressure of 10 pounds per square foot is assumed, then a lower speed than circular (25,000 feet per second) is not permissible at 293,000 feet altitude (cf. Section IV). Consequently, if the constrained path is to be extended somewhat into the range of positive (supporting) lift, a lower initial altitude is necessary. The minimum velocity, at which q becomes 10 pounds per square foot, is then given as a function of altitude, expressed by the density ratio

$$V = \sqrt{\frac{2q}{\sigma \rho_{oo}}} \qquad = \sqrt{\frac{841}{\sigma}} \, q \; \text{- - - - - - - - - - - - - - - -} \quad (39)$$

The resulting altitude - minimum velocity correlation is shown in Figure 25. The same graph also contains the ratio of lift coefficient over lifting area load (lift parameter) required to hold the vehicle at the particular altitude and at the minimum speed. The lift parameter is given by (cf. Section IV)

$$\frac{C_L}{W/S} = 6 \times 10^{-14} \cdot \frac{r}{\sigma} \left(\frac{\gamma}{v^2 r} - 1 \right) \text{- - - - - - - - -} \quad (40)$$

FIG. 24 DYNAMIC PRESSURE VS. ALTITUDE FOR DIFFERENT VELOCITIES

FIG. 25 MINIMUM FLIGHT VELOCITY FOR
q = 10 LB/FT² AS FUNCTION OF ALTITUDE
AND
LIFT PARAMETER REQUIRED FOR THE
RESPECTIVE SPEED-ALTITUDE COMBINATION

VELOCITY ~ 1000 FT/SEC.

ALTITUDE ~ 1000 FT.
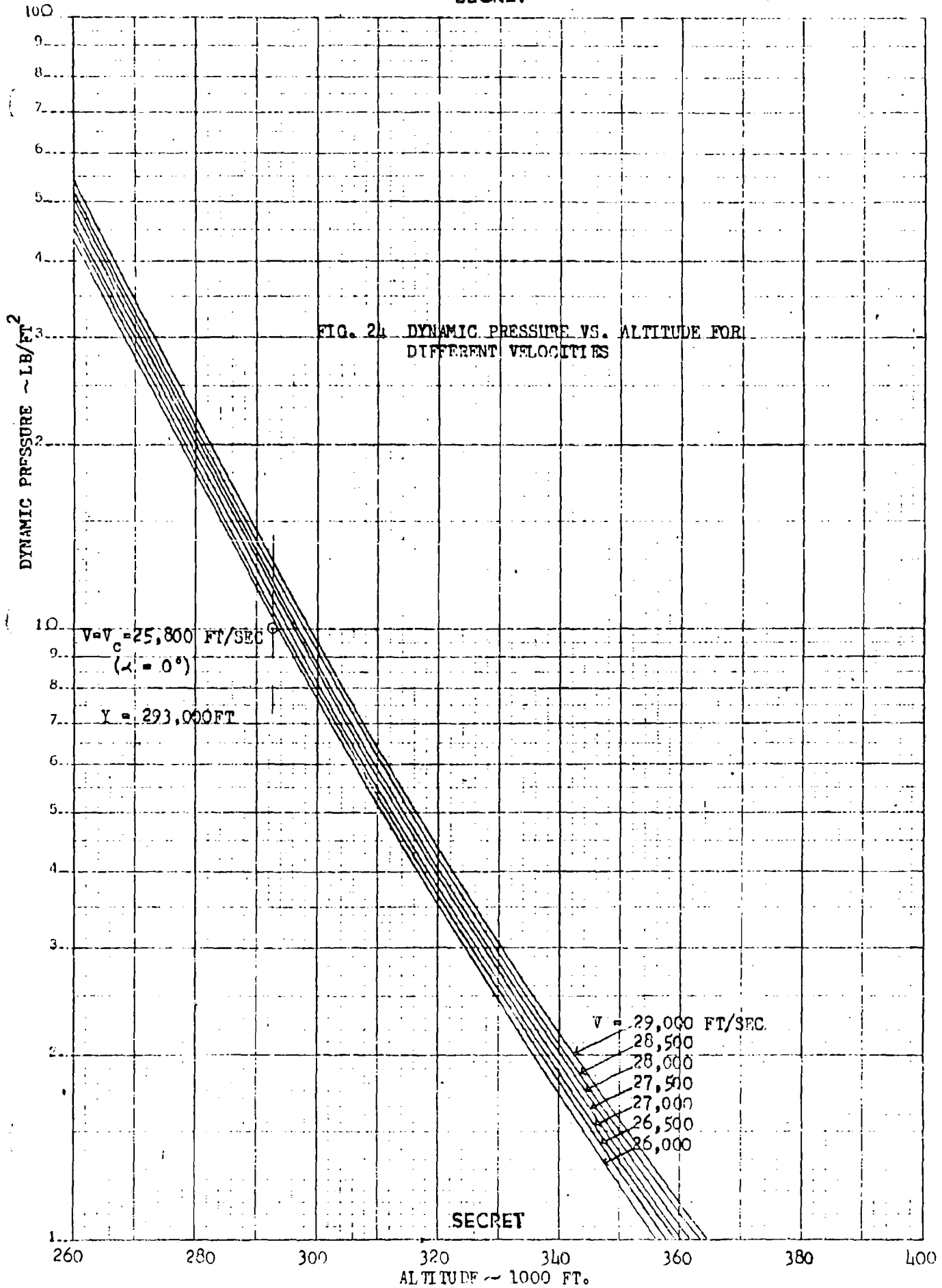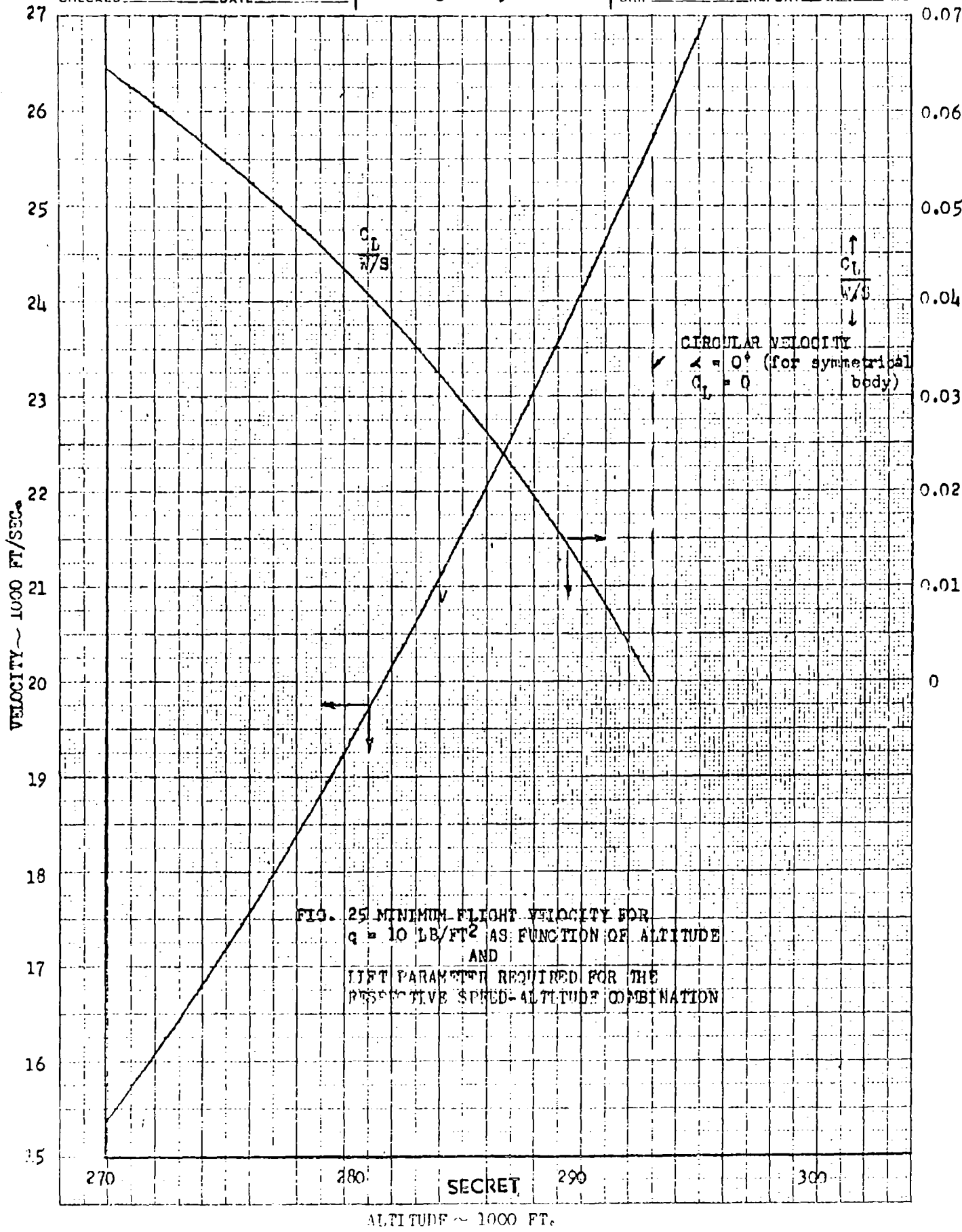
SECRET

BELL *Aircraft* CORPORATION

y —————————————— Date ——————————

hecked ——————————— Date ————————

Model —————————— Page ____53____

Missile

Airplane ——————— Report _D143-945-014_

If a lifting area load of the order of 20 pounds per square foot is assumed, only a very small value for $C_L/W/S$ will result, since C_L will be small. Thus, even with very small lifting area loads, it appears difficult to place the initial altitude much below 293,000 feet in the hope of thereby extending the constrained path below circular speed.

It may be emphasized at this point that the preceding considerations are based on a velocity-altitude correlation which satisfies the condition that q = 10 pounds per square foot. The results show that, although this dynamic pressure may satisfy aerodynamic controllability requirements, it obviously does not satisfy aerodynamic glide requirements, because the high lift coefficient which is obtained at the technically feasible lifting area loads, probably cannot be produced. This result, then, is in accord with the findings in Section IV which also showed that the aerodynamic equilibrium glide altitude is lower than the altitude where q = 10 pounds per square foot for the particular speed, namely, where q is about 3 times as much, e.g., at 270,000 feet for 24,000 feet per second if C_L = C.1 and W/S = 20.

The flight time and the range during motion in the constrained path follows from integration of the equations

$$\frac{d^2s}{dt^2} = \frac{dv}{dt} = -\frac{D}{m} = -\frac{g\rho}{2}\frac{S}{W} C_D v^2$$

$$= -\frac{g_{oo}\rho_{oo}}{2} \sigma \frac{S}{W} C_D v^2 \qquad - - - \cdot - - - \cdot \quad (41)$$

$$= -\sigma' \frac{S}{W} C_D v^2$$

using the relation

$$-v\frac{d\theta}{dt} = \frac{L}{m} - g \left(1 - \frac{v^2 r}{\gamma}\right) = 0 \qquad - - - - - - - - \quad (42)$$

since, for constant flight altitude $d\theta$ /dt = 0.

Best Available Copy

A correct integration of the preceding equation leads to lengthy relations for flight time and range. A simplified solution yields

$$\text{time interval} \quad \Delta t = \frac{1}{\sigma' C v_i} \left(\frac{1}{v} - \frac{1}{v_i} \right) \quad - - - - - - \quad (43)$$

flight path length

$$\Delta s = \frac{1}{\sigma' C} \ln (1 + \sigma' C v_i \, \Delta t) \quad - - - - - - - - - \quad (44)$$

and corresponding range on surface

$$\Delta x = \Delta S \, \frac{r_{oo}}{r_i} = \frac{1}{\sigma' C} \, \frac{r_{oo}}{r_i} \ln (1 + \sigma' C \, v_i \, \Delta t) \quad (45)$$

where r_i is the initial (constrained path) altitude and r_{oo} the radius of the earth and where the two terms

$$\sigma' = \frac{\sigma g_{oo} \rho_{oo}}{2} \quad \text{lb/ft}^3 = 3.829 \times 10^{-2} \sigma \quad - - - - \quad (46)$$

and

$$C = \frac{C_L}{\frac{W/S}{L/D}} \quad \text{ft}^2/\text{lb} \quad - - - - - - - - - - - - - - - \quad (47)$$

are assumed to be constant for the respective integration interval, Δt, v is the instantaneous velocity, v_i is the initial speed with which the vehicle is delivered into the constrained path, Δt is the time interval required for slowing down the vehicle from v_i to v and Δs and ΔX are the corresponding path-length and surface-range increments. For a given flight altitude, σ' is fixed and stays constant in a constrained path, because y = constant. Thus Δt, Δs, and ΔX increase inversely proportional to C. This value, therefore, should be small. In other words, L/D should be much larger than $C_L/(W/S)$. This means, as was to be expected, for a path determined by aerodynamic forces, that the range depends essentially on getting as high an L/D as possible for as small a C_L as possible.

BELL Aircraft CORPORATION

Model —

Missile

Airplane —

Page 55

Report D143-945-014

As the vehicle moving with $v_i > v_c$ loses speed, $C_L/(W/S)$ decreases (α decreases) until, at $v = v_c$ the lift parameter must be zero (α = zero for symmetrical profile). The variation of L/D depends on the range of angle of attack between v_i and v_c. If α_i was much larger than the angle of attack α_{opt} for maximum L/D, then L/D will at first increase with decreasing speed until α_{opt} is reached. Thus, for $\alpha_i >$ $\alpha > \alpha_{opt}$, L/D increases while $C_L/(W/S)$ decreases. Therefore C decreases rapidly. For $\alpha < \alpha_{opt}$, L/D decreases like $C_L/(W/S)$. In this range, then, C must change much less or even stay approximately constant. At $v = v_c$ both $C_L/(W/S)$ and L/D are zero — hence, C is indeterminate. Physically, there is no longer a force normal to the flight path; there is only drag. For somewhat more accurate determination of the constrained path data, an iterative process must therefore be applied. In the first rough approximation, however, a constant mean value for C can be assumed. C must be a rather small value. Assuming $C = 10^{-2}$ one obtains the surface range and the flight time as a function of the initial velocity and the flight altitude. For any other C the range and flight time become

$$\Delta X' = \Delta X \frac{10^{-2}}{\overline{C}'} \quad - - - - - - - - - - - - - - - - - \quad (48)$$

$$\Delta t = \Delta t \frac{10^{-2}}{\overline{C}'} \quad - - - - - - - - - - - - - - - - - \quad (49)$$

that is, range and flight time are proportional to $\overline{C}$. It can be seen that the ranges obtained are comparatively small. For instance, having v_i = 29,000 feet per second, and staying in the constrained path down to 24,500 feet per second yields a range of about 4,900 nautical miles. With the residual speed, a range of about 16,000 nautical miles is obtained along an $(L/D)_{max}$ glide path. Adding a range of approximately 1000 nautical miles for the powered ascent,[*] yields then a total of 21,900 nautical miles, that is, just one circumnavigation. This estimate is crude, but it shows rather definitely that more than one revolution does not appear feasible, even if one assumes $\overline{C}$ values as low as 2×10^{-3} to 5×10^{-3} — values which are not likely to be achieved.

The basic result is therefore that the constrained path cannot be used for more than one circumnavigation. Although the exact initial velocity required for this operation must be determined by a more detailed investigation, it appears nevertheless that it lies considerably above

[*] The range gained during powered ascent will be very long due to the very high cut-off velocity.

circular velocity, probably somewhere between 28,000 and 30,000 feet per second. The local circular velocity is about 25,800 feet per second. Using $v_1 = 0.89$ yields $\frac{25,800}{0.89} = 29,000$. It is then necessary to add 28,000 - 25,800 = 2,200 feet per second or 30,000 - 25,800 = 4,200 feet per second, assuming that the elliptic excess is produced without losses. Thus, the over-all velocity potential of the vehicle must be 29,000 + 2,200 = 31,200 to 29,000 + 4,200 = 33,200 feet per second.

The conclusions which must be drawn from these results are that the very high energy requirement of the constrained path for as little as one circumnavigation renders this type of path technically unattractive, at least with chemical rocket engines, independent of other features such as exclusively aerodynamic control, constant flight altitude at super-circular speed, weight throughout the flight, all of which might be considered to be advantageous.

SECRET

| By | Date | | Model | Page | 57 |
| Checked | Date | BELL Aircraft CORPORATION | Missile Airplane | Report | D143-945-014 |

VIII. PATH TYPE IV: SUSTAINED

In the sustained path the vehicle cruises at constant speed and altitude with the aid of a sustainer motor used to overcome the drag encountered at the particular speed and angle of attack of the body.

Obviously, if the altitude is considerably above 100,000 feet and the velocity is much larger than about 4,000 ft/sec, the sustaining thrust must be produced by a rocket engine. Therefore, minimization of the propellant consumption during the cruise is of great importance. An additional important parameter from the viewpoint of the over-all vehicle is the take-off weight.

As far as vulnerability is concerned, it makes little difference whether the vehicle flies at 15,000, 20,000 or 25,000 feet per second. In all cases the speed and the associated altitude are high enough to frustrate even advanced air defense systems. The investigation of the sustained path should therefore comprise circular as well as subcircular velocities.

At circular velocity no lift is required. The deceleration (in surface g-units) due to the drag follows therefore from

$$- \frac{dv}{dt} \times g_{oo} = \frac{D}{m} \ - - - - - - - - - - - - - - - - \quad (50)$$

where D is in pounds

$$- n = \frac{D}{W} = \frac{\rho_{oo}}{2} \sigma \, v^2 \ C_D \ \frac{S}{W} = \frac{\sigma v^2 \ \frac{S}{W}}{841} \ C_D - \quad (51)$$

where, in the case of circular velocity, v is given by $\sqrt{\gamma/r}$. The dynamic pressure as well as (-n) for $W/S = 20$ and $C_D = 0.7$ are presented as a function of the altitude in Figure 20. Based on this information and on a "lower limit" information with $C_D = 0.35$, the thrust and propellant consumption per second are found from

$$F = - n \times W \ - \quad (52)$$

$$\dot{w} = \frac{F}{F_{sp}} \ - - - - - - - - - - - - - - - - - - - \quad (53)$$

where F is the thrust, W is the vehicle weight, F_{sp} is the specific thrust, and $\dot{w}$ is the propellant consumption per second. The propellant consumption per revolution follows from

$$w_r = \dot{w} t_r \quad\text{-----------------} \quad (54)$$

where t_r is the period of revolution which obtains for different altitudes

y (ft)	300,000	400,000	500,000	600,000
t_r (sec)	5,200	5,250	5,300	5,350

For $W = 10,000$ pounds and $F_{sp} = 350$ pounds thrust per second per pound of propellant and using the earlier information regarding n, the propellant consumption per revolution is obtained as shown in Figure 26. It can be seen that from about 450,000 feet altitude on upward, the propellant consumption per revolution is so small that several revolutions appear feasible without obtaining an unduly heavy upper stage.

In order to account for the change in vehicle weight during the cruise, the equation of weight decrease with time (Equation (53))

$$\frac{dW}{dt} = -\frac{F}{F_{sp}} = -\frac{n_0\,W}{F_{sp}}$$

where

$$-n_0 = \frac{F_0}{W_0} = -n$$

(the subscript zero indicating initial conditions) must be integrated to yield

$$\ln \frac{W_0}{W_1} = \frac{n_0}{F_{sp}} t_1 \quad\text{---------------} \quad (55)$$

The burning time t_1 is of course equal to t_r, assuming that, after termination of the (powered) cruise at circular velocity at 450,000 feet, the vehicle is capable of gliding one more time around the earth. Figure 27

ASSUMPTIONS

VEHICLE WEIGHT: 10,000 lb
LIFTING AREA LOAD: 20 lb PER SQ FT
SPECIFIC THRUST: 350 SEC
DRAG COEFFICIENT BASED ON LIFTING
AREA (FREE MOLECULE FLOW)

$C_D = 0.7$

$C_D = 0.35$
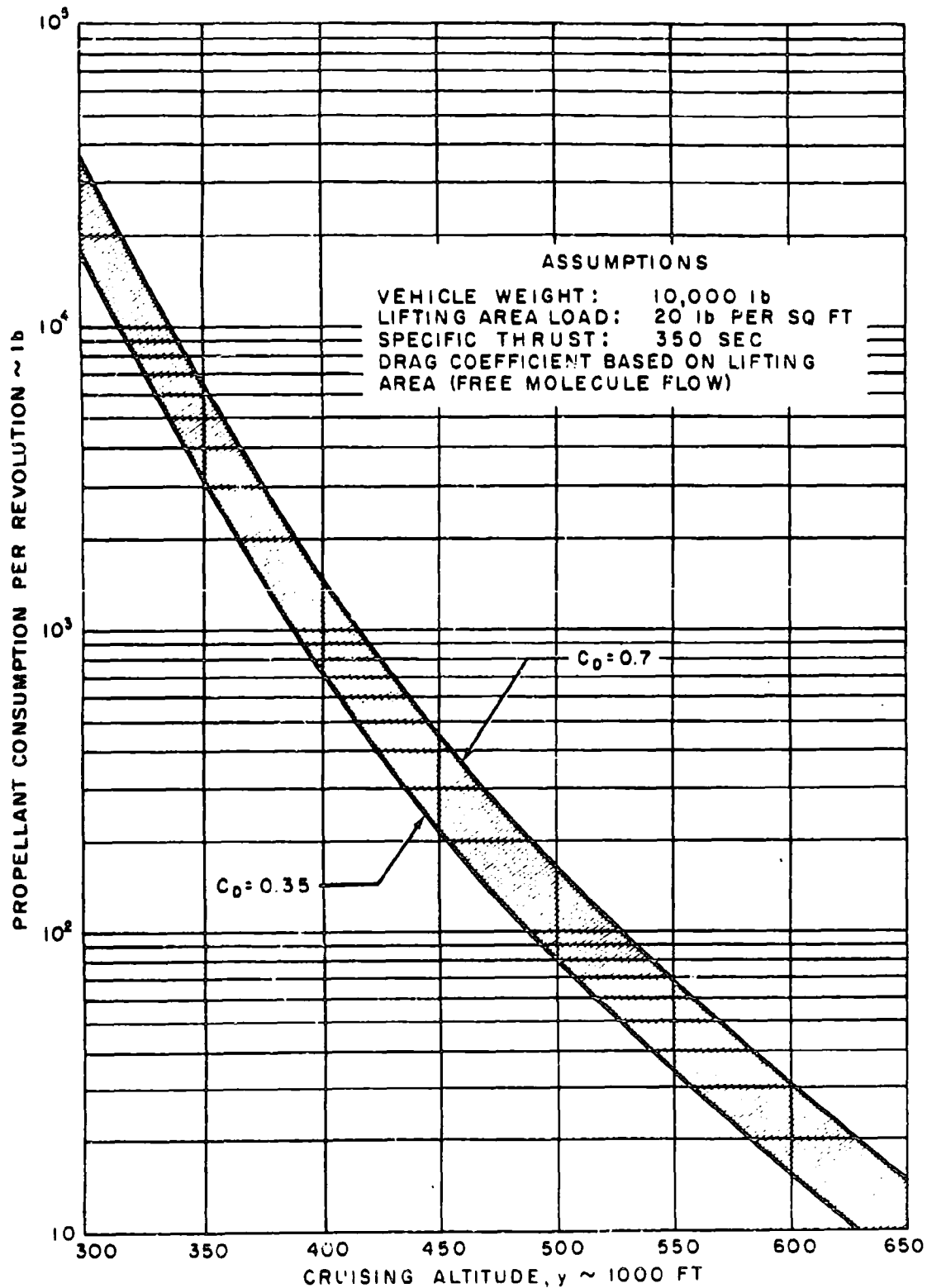
Figure 26. Sustained Path - Approximate Propellant Consumption
per Revolution vs Cruising Altitude
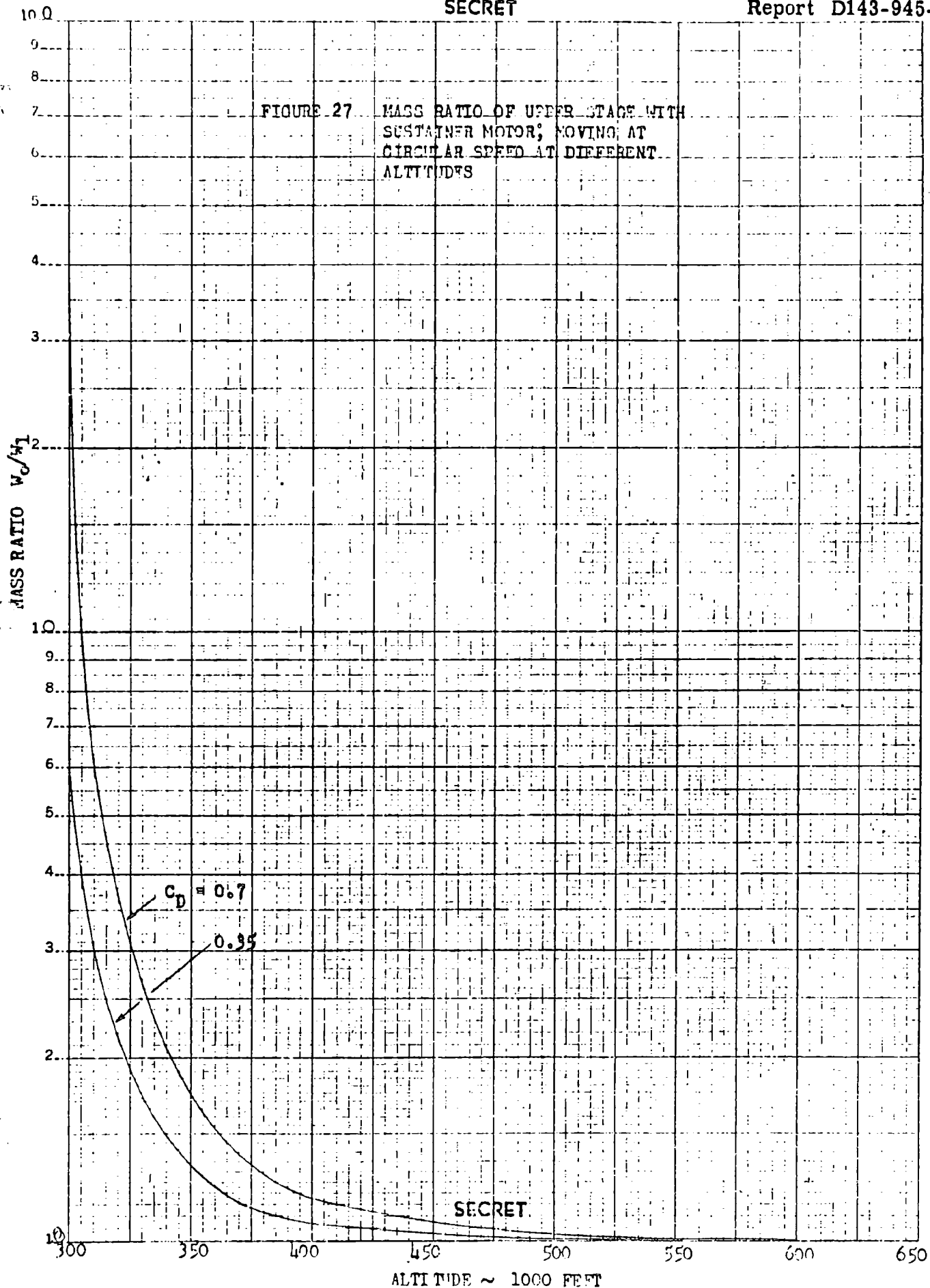
Form E4-1 Rev. 353

FIGURE 27   MASS RATIO OF UPPER STAGE WITH
SUSTAINER MOTOR, MOVING AT
CIRCULAR SPEED AT DIFFERENT
ALTITUDES

$C_D = 0.7$

0.35

SECRET

ALTITUDE ~ 1000 FEET

MASS RATIO w_c/w_1

shows the mass ratios obtained for the upper stage as a function of y for two values of C_D. This mass ratio as well as some additional values are presented in Table I. The tremendous increase in weight with decreasing altitude below 350,000 feet as well as the great difference in propellant consumption due to the final weight W, will be noted. The two values for W_1 correspond approximately to that of the upper stage of MX-2276 (15,000 pounds) and to a wingless glider (surfboard-type) upper stage of about equal performance. It is apparent that flight altitudes between 400,000 and 450,000 feet are necessary in order to arrive at technically feasible and reasonable upper stage weights. If an altitude of 450,000 to 500,000 feet is selected, the take-off weight for several circumnavigations will be about the same as in the case of the spiral path.

It may be pointed out that the values given in Table I and plotted in Figure 27 refer to one revolution. The values W_o/W_1, W_o for a given W_1 and the propellant consumption per revolution w_r are obtained easily for i revolutions by multiplying the natural logarithm of the mass ratio by i. Therefore, $\ln W_o/W_1$ has also been tabulated.

For operation at less than circular velocity the vehicle must rely on lift for its cruise. The lift, L, must be equal to the apparent weight, W_{app}. In order to express the deceleration (in g_{oo}) in terms of L/D we can write

$$-n \, W = D = \frac{L}{L/D} = \frac{W_{app}}{L/D} \quad - - - - - - - - - - - - - (56)$$

whence

$$-n = \frac{W_{app}/W}{L/D} \quad - - - - - - - - - - - - - - - - - (57)$$

| By | Date | **BELL** *Aircraft* CORPORATION | Model | Page | **62** |
| Checked | Date | | Missile
Airplane | Report | D143-945-014 |

TABLE I. VEHICLE DATA FOR SUSTAINED FLIGHT AT CIRCULAR SPEED

	300,000	400,000	500,000	600,000
y (ft)	300,000	400,000	500,000	600,000
$C_D = 0.7$				
$-n \, (g_{oo})$	0.244	0.0101	0.00112	0.000205
$\ln W_o/W_1$	3.624	0.1512	0.01696	0.003129
W_o/W_1	37.337	1.163	1.017	1.0031
$^*\Lambda$	0.973	0.14	0.0167	0.00309
W_o when $W_1 = 10,000$ lb	373,370	11,630	10,170	10,031
W_o when $W_1 = 15,000$ lb	559,950	17,455	15,255	15,046
w_r (lb/rev) 10,000	363,370	1,630	170	31
15,000	544,950	2,455	255	46
$C_D = 0.35$				
$n(g_{oo})$	0.122	0.00505	0.000506	0.0001025
$\ln W_o/W_1$	1.812	0.0756	0.00848	0.0015645
W_o/W_1	6.123	1.0785	1.00854	1.0016
$^*\Lambda$	0.8367	0.0728	0.008468	0.0016
W_o when $W_1 = 10,000$ lb	61,230	10,785	10,086	10,016
W_o when $W_1 = 15,000$ lb	91,845	16,177	15,128	15,024
w_r (lb/rev) 10,000	60,230	785	86	16
15,000	90,345	1,177	128	24

$^*\Lambda$ = ratio of useful propellant to gross weight of vehicle or stage

For one full circumnavigation the following values are obtained (Table II) using the tabulated values for glide altitude and L/D:

TABLE II. SUSTAINED PATH DATA FOR SUBCIRCULAR SPEED

v (ft/sec)	22,000	20,000	18,000	16,000	14,000	12,000
V (n. mi./sec)	3.63	3.3	2.97	2.65	2.31	1.98
y (10^{-3} ft)	240,000	200,000	180,000	165,000	155,000	146,000
L/D	3.73	4.5	4.8	4.8	4.9	5.0
W_{app}/W	0.25	0.4	0.5	0.6	0.7	0.78
$-n$ (g_{00})	0.067	0.089	0.104	0.125	0.143	0.156
F_{sp} (sec)	350	350	350	350	350	350
t_r (sec)	6,000	6,550	7,280	8,190	9,350	10,900

If only one circumnavigation is considered, the glide range X_G at the given speed after termination of the sustained path must be taken into account. The range for which sustained operation is required becomes then $X_s = 21,600 - X_G{}^*$, and from this results the period t_s of sustained operation. From this follow the pertinent vehicle data as before. The relevant data are compiled in Table III.

---

* Neglecting the slight increase (about 2%) of the path length due to flight altitude.

TABLE III. VEHICLE DATA FOR SUSTAINED FLIGHT AT SUBCIRCULAR SPEED

(For 1 Revolution)

V (ft/sec)	22,000	20,000	18,000	16,000	14,000	12,000
X_G (n. mi.)	10,600	8,000	6,000	4,500	3,250	2,300
X_S (n. mi.)	11,000	13,600	15,600	17,100	18,350	19,300
t_S (sec)	3,030	4,121	5,252	6,453	7,944	9,747
$\ln W_O/W_1$	0.5757	1.0467	1.56	2.304	3.241	4.344
W_O/W_1	1.777	2.849	4.758	10.014	25.53	76.7
W_O when W_1= 10,000 lb	17,770	28,490	47,580	100,140	255,300	767,000
W_O when W_1= 15,000 lb	26,655	42,735	71,370	150,210	382,950	1,150,500
$\dot{w}$ (lb/t_S) 10,000	7,770	18,490	37,580	90,140	245,300	757,000
15,000	11,655	27,735	56,370	135,210	367,950	1,135,500

Form E6-1 Rev. 353

By	Date	BELL *Aircraft* CORPORATION	Model	Page 65
Checked	Date		Missile / Airplane	Report D143-945-014

The mass ratio is plotted in Figure 28. It shows the same steep gradient as in the case of the sustained path at circular velocity. The glide range X_G in Table III refers to glide at maximum L/D. The propellant consumption w during the sustained portion of the path represents, therefore, the minimum, or most favorable, value. It can be seen, for instance, that in the case of 22,000 feet per second initial velocity, it is necessary for global capacity to have about 11,000 pounds propellant more on board than used for the MX-2276. Making the rough assumption that for each additional pound in the upper stage the take-off weight is increased by about 40 pounds, this means an increase in take-off weight by about 465,000 pounds. With $(F_2 + O_2)$ - JP-4 as propellants, the present MX-2276 weighs about 550,000 pounds. To increase its capacity to a global level by letting it cruise along a sustained path at 22,000 feet per second brings the weight, therefore, to roughly one million pounds. This is the same order of magnitude as for a global vehicle following a spiral path or a sustained path at circular velocity, as will be seen in Section IX. However, because the order of magnitude is the same, a more detailed investigation is required to compare more accurately a temporarily sustained MX-2276 of global capacity with a global weapon system using the spiral or the circular velocity sustained path.

To go to lower velocities does not appear attractive. The large increase in propellant consumption apparently outweighs all effects of a performance reduction of the lower stages due to smaller cruising speed.

From these investigations it can be concluded that the sustained circular-velocity path compares favorably with the other global flight paths discussed before, and that it may be possible without significant penalty (if any penalty at all) to use a partly sustained path at lower speed ($\geq$ 22,000 feet per second), and finally that a partly sustained path at velocities below about 22,000 feet per second does not appear promising owing to the intensification of aerodynamic heating in this region and the increase in propellant weight required for the duration of sustained operation.

SECRET

FIGURE 28 MASS RATIO OF UPPER STAGE WITH
SUSTAINER MOTOR AS FUNCTION OF
FLIGHT SPEED

MASS RATIO W_o/W_1
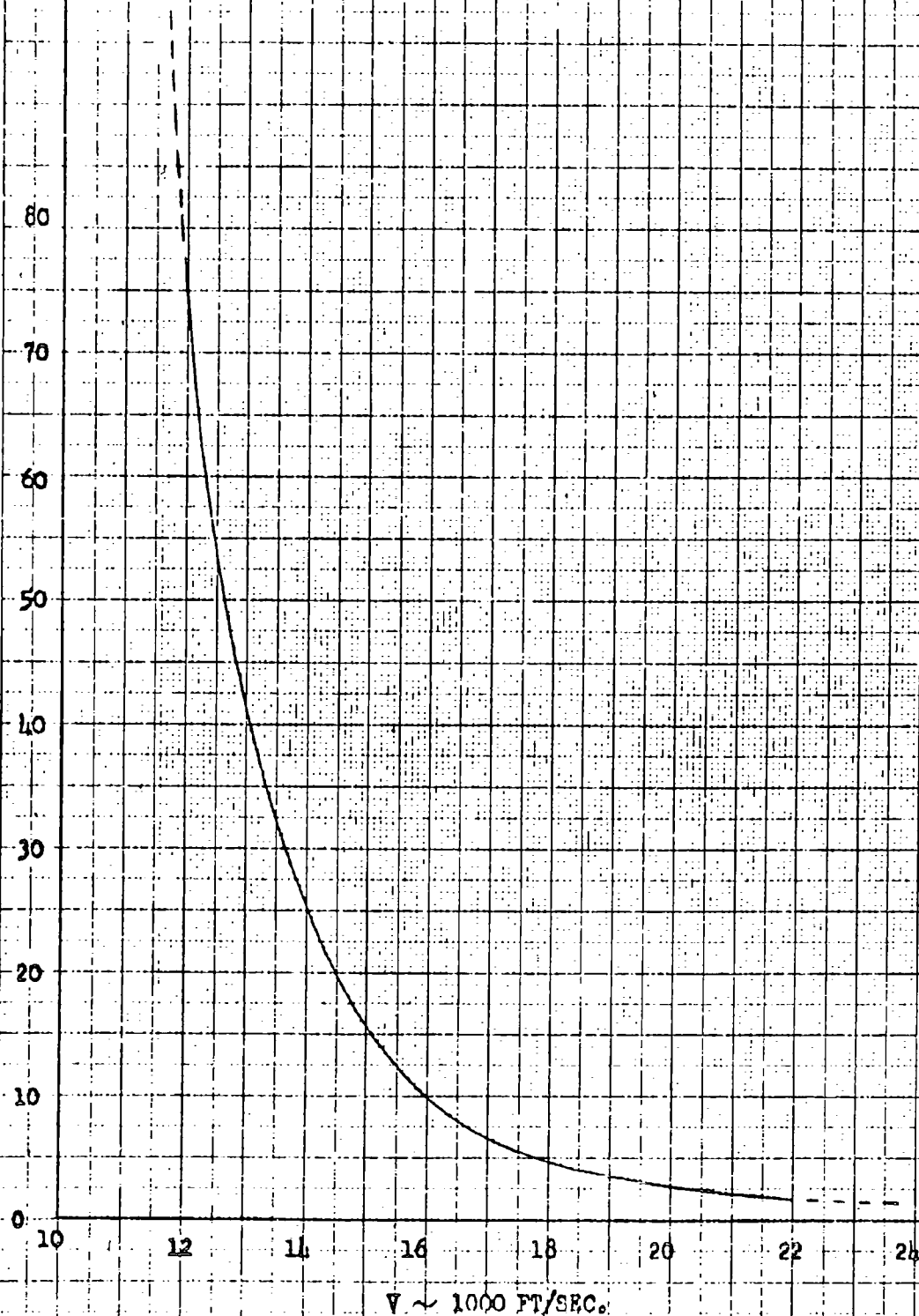
$V \sim 1000$ FT/SEC.

IX. DISCUSSION OF GLOBAL WEAPON SYSTEM PATHS

It is now possible to summarize the essential characteristics of the flight path types I through IV on the basis of the results gained in the preceding sections. The information is presented in Table IV, and has been evaluated in order to arrive at a first appraisal of the relative merits of these flight paths.

The energy requirement, based on the number of revolutions assumed, is given in terms of the ideal velocity. Assuming that the total energy required to send the given rest mass m over the respective flight path is expressed in terms of equivalent kinetic energy, then the ideal velocity is defined by $\frac{m}{2} v_{id}^2$ = kinetic energy of rest mass + potential energy of rest mass + energy lost due to gravitational pull during powered flight + energy lost due to drag + energy lost due to steering.

Therefore, v_{id} represents the velocity which the vehicle could obtain under the ideal, loss-free conditions of propulsion in a gravity-free vacuum. This is the velocity for which the over-all mass ratio of the vehicle must be laid out. Table IV shows that the energy requirements are about the same for all paths, with the exception of the constrained path.

For ignition and power plant operation, the number of individual propulsion periods is of importance. It is desirable to keep this number at a minimum for reasons of efficiency, and reliability of the ignition process. In this respect, the elliptic path is less favorable, because it requires a second propulsion period at the apogee.

The characteristic flight path conditions indicate extreme altitude for the elliptic path and extreme speed for the constrained path.

The conditions over the target area are most favorable for the spiral path which permits the lowest altitude and speed without, however, rendering the vehicle vulnerable to enemy defense. The elliptic and constrained paths show near-circular velocity over the target area at an altitude of about 300,000 feet. It is assumed in this case that the constrained path leads directly to the target area. If it leads in the opposite direction, as in the case of the spiral and the ellipse, the constrained path conditions over the target area are similar to those of the MX-2276. An altitude of 300,000 feet may be regarded as the upper limit for the radar reconnaissance equipment used in the MX-2276, if it is to give a resolution comparable to that expected from the MX-2276. The highest altitude over the target area is obtained from the sustained path.

| By _____ Date _____ | **BELL** *Aircraft* CORPORATION | Model _____ Missile Airplane _____ | Page __68__ |
| Checked _____ Date _____ | | | Report D143-945-014 |

TABLE IV. FLIGHT PATH CHARACTERISTICS FOR GLOBAL WEAPON SYSTEM

Subject Field	Parameter	Spiral	Elliptic	Path Constrained	Sustained (Circular Velocity)
Energy Requirement	Number of Revolutions	1	1	1	2
	Ideal Velocity (10^3 fps)	29-30	30	32-33	29-30
Ignition and Power Plant Operation	Propulsion Periods	1	2	1	Continuous (Decreasing Thrust)
Characteristic Flight Conditions	Initial Velocity (10^3 fps)	25.7	25-25.7	28-29	25.7
	Maximum Velocity (10^3 fps)	25.7	26-26.5	28-29	25.7
	Maximum Altitude (10^3 ft)	400-450	700-1000	290-300	450
Conditions over Target Area	Velocity (10^3 fps)	18-16	26	26-25	25.7
	Altitude (10^3 ft)	200-180	300	300-290	450
Load Conditions	Normal Load During Coasting or Cruise (g)	0-1	0-1	-0.2-1	0-1
Stability and Control	Control Systems	Dual	Dual	Aerodynamic	Dual

The load conditions normal to the instantaneous flight path direction, resulting from the flight path configuration proper (i.e., excluding load conditions during powered flight or due to maneuvering), are small in all cases and never anywhere near the values obtained for the skip path. The negative sign in the case of the sustained path indicates that, during flight at greater than circular velocity, the apparent weight vector points away from the center of the earth.

With respect to stability and control requirements, the number of control systems needed is indicative of the weight, and relative complexity as well as reliability to be expected. Obviously, a vehicle operating inside and outside the relevant atmosphere must have two types of control, aerodynamic control within the atmosphere, and jet control or inertial attitude control by means of gyroscopes or flywheels for vacuum flight. The dual control is required for all paths, except the constrained path or a sustained path at velocity lower than circular.

By _____ Date _____
Checked _____ Date _____

BELL Aircraft CORPORATION

Model _____   Page   70
Missile
Airplane _____   Report D143-945-014

X. VEHICLE WEIGHT AND CONFIGURATION

A preliminary study of the take-off weight of the global weapon system has been conducted in order to evaluate the energy requirements of the previously discussed flight paths in terms of vehicle weight. Because trends appear more significant at this state of the study and presently are more readily obtainable than detailed component weight determinations, some simplifications have been made which will be outlined subsequently.

The weight of each stage has been broken down into dry weight (airframe engine installations) W_d, propellant weight serving the acceleration of the vehicle in flight direction, W_Δ , propellant weight for auxiliary purposes (turbine pump), W_α , residual propellant left in tanks after cut-off, W_ρ , and payload weight W_λ ; with $W_p = W_\Delta$ $+ W_\alpha$ $+ W_\rho$ it then is

$$W_d + W_p + W_\lambda \ = W_o$$

W_λ for lower stages is the sum of all upper stages; for the upper stage a payload weight W_λ of 4200 pounds has been assumed, the same as for the present MX-2276.

The following loss factors for the propulsion phase of the individual stages have been assumed throughout the investigation

Stage 1 $\dfrac{\Delta v}{\Delta v_{id}}$ = $(\xi_v)_1$ = 0.75

Stage 2 $(\xi_v)_2$ = 0.94

Stage 3 $(\xi v)_3$ = 0.98

These values are reasonable averages obtained from a number of trajectory calculations. The resulting over-all velocity factor is 1/3 (0.75 + 0.94 + 0.98) = 0.89. This value gives the correct magnitude for the losses encountered during the propulsion period. The simplification

By _____ Date _____
Checked _____ Date _____
BELL Aircraft CORPORATION
Model _____
Missile
Airplane _____
Page ___71___
Report __D143-945-014__

lies in the fact that, keeping the individual stage loss factors constant, means maintaining about the same trajectory in view of a large range of cut-off velocities considered. As a result, the cut-off altitudes will vary for the different cases. The Λ and W_T/W_O values resulting from the preceding loss factors are shown in Figure 29 for the three stages, as functions of the actual cut-off velocity, using the following propellants and specific impulses: (50% F_2 + 50% O_2) - JP-4; mixture ratio by weight, r = 3.5; chamber pressure, p_c = 1000 psia; I_{sp_1} = 316 seconds for Stage 1 (exit pressure p_{e_1} = 10.6 psia); and I_{sp_2} = I_{sp_3} = 361 seconds (p_{e_2} = p_{e_3} = 1.47 psia) for second and third stage. (The values of I_{sp_2} and I_{sp_3} used were incorrectly reported to be 349 seconds in Ref. 8).

Finally, a simplification has been made by assuming a constant ratio of dry weight to gross weight in spite of considerable variations in take-off weight. The values $(W_d/W_O)_1$ = 0.20 and $(W_d/W_O)_2$ = 0.15 have been selected on the basis of general design considerations, assuming a winged first stage and a nonwinged second stage. For the third stage, different values $(W_d/W_O)_3$ have been assumed to explore the effect of the gross weight of the upper stage on the over-all take-off weight.

By varying the velocity increment of the second and third stages for a given first stage velocity increment, and by repeating this for three different first stage velocity increments, three curves are obtained for a given over-all cut-off velocity, e.g., $(\Delta v)_{tot}$ = 25,700 feet per second. By doing this for different over-all cut-off velocities, a number of sets of three curves is obtained. They are presented in Figures 30 through 32, for three different values of $(W_d/W_O)_3$. Figure 31 also shows the associated weights of the second and third stages. The weights are plotted against the third stage velocity increment. The location of the minima indicates a trend toward lower take-off weights with decreasing first stage velocity increment, down to about 5700 feet per second. From the viewpoint of recovery economy it is significant to note that with decreasing first stage velocity increment the weight of the second stage goes up, hence more hardware must be thrown away at the lower take-off weight. This is a generally valid trend, inherently connected with multistage rocket vehicles. The more hardware is made expendable the lower will be the take-off weight, all other conditions being the same.

From these graphs the weight curves in Figure 33 have been obtained, showing four bands of over-all take-off weights for four different values of W_d/W_O of the third stage, plotted versus the actual velocity of

SECRET

FIGURE 29 RATIO OF PROPELLANT WEIGHT TO TOTAL WEIGHT AS A FUNCTION OF
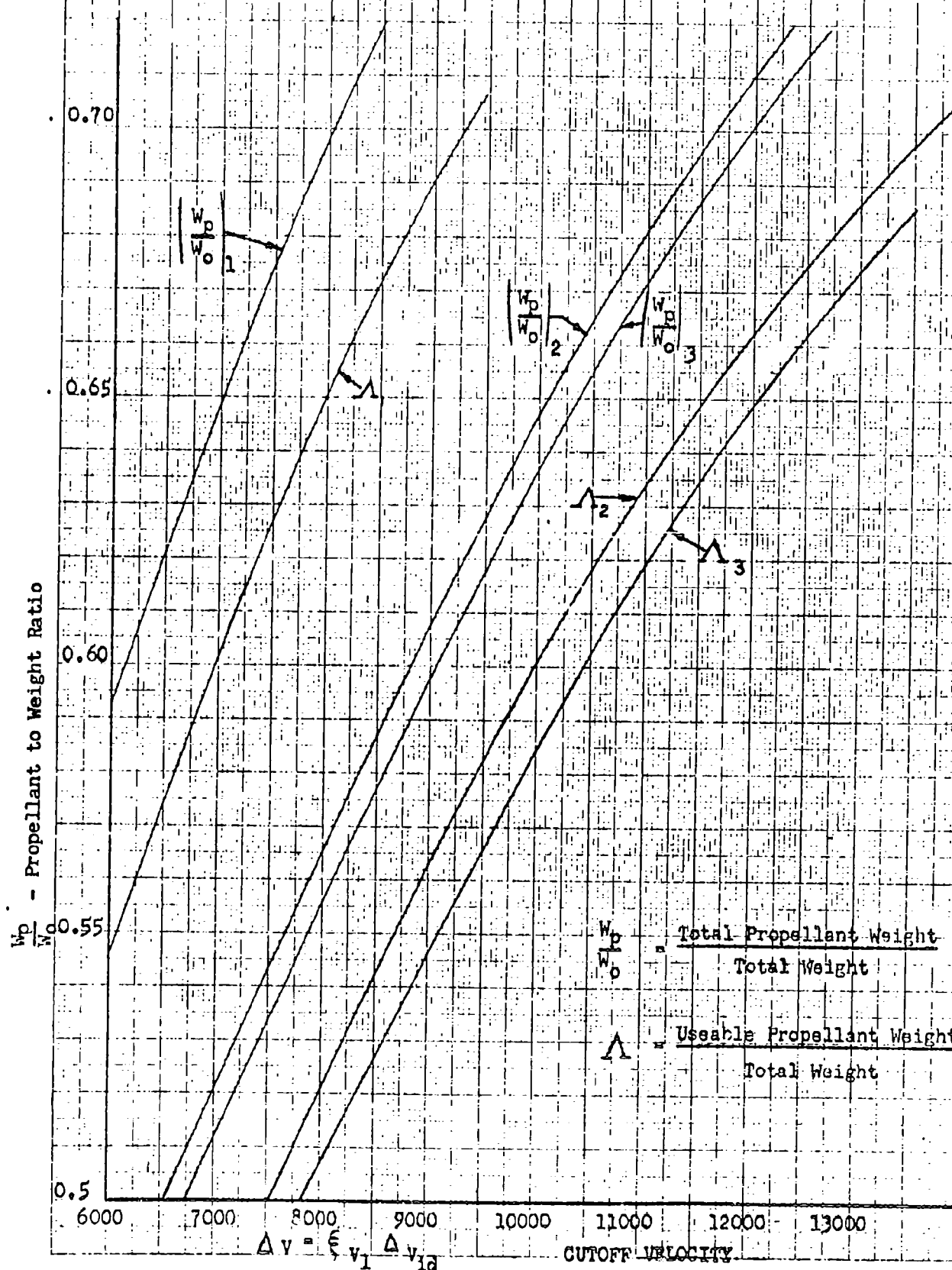ACTUAL CUT OFF VELOCITY FOR ALL 3 STAGES

$$\frac{W_p}{W_o} = \frac{\text{Total Propellant Weight}}{\text{Total Weight}}$$

$$\Lambda = \frac{\text{Useable Propellant Weight}}{\text{Total Weight}}$$

$\frac{W_p}{W_o}$ – Propellant to Weight Ratio

$\Delta V = \xi_{V_1} \Delta_{V_{1d}}$ CUTOFF VELOCITY

SECRET

SECRET
BELL *Aircraft* CORPORATION

MODEL _____ PAGE 73
SHIP _____ REPORT D143-945-014

BY _____ DATE _____
CHECKED _____ DATE _____

FIGURE 30 - EFFECT OF ENERGY DISTRIBUTION AMONG THE STAGES ON TAKE-OFF HEIGHT

Figure 31. Effect of Energy Distribution Among the
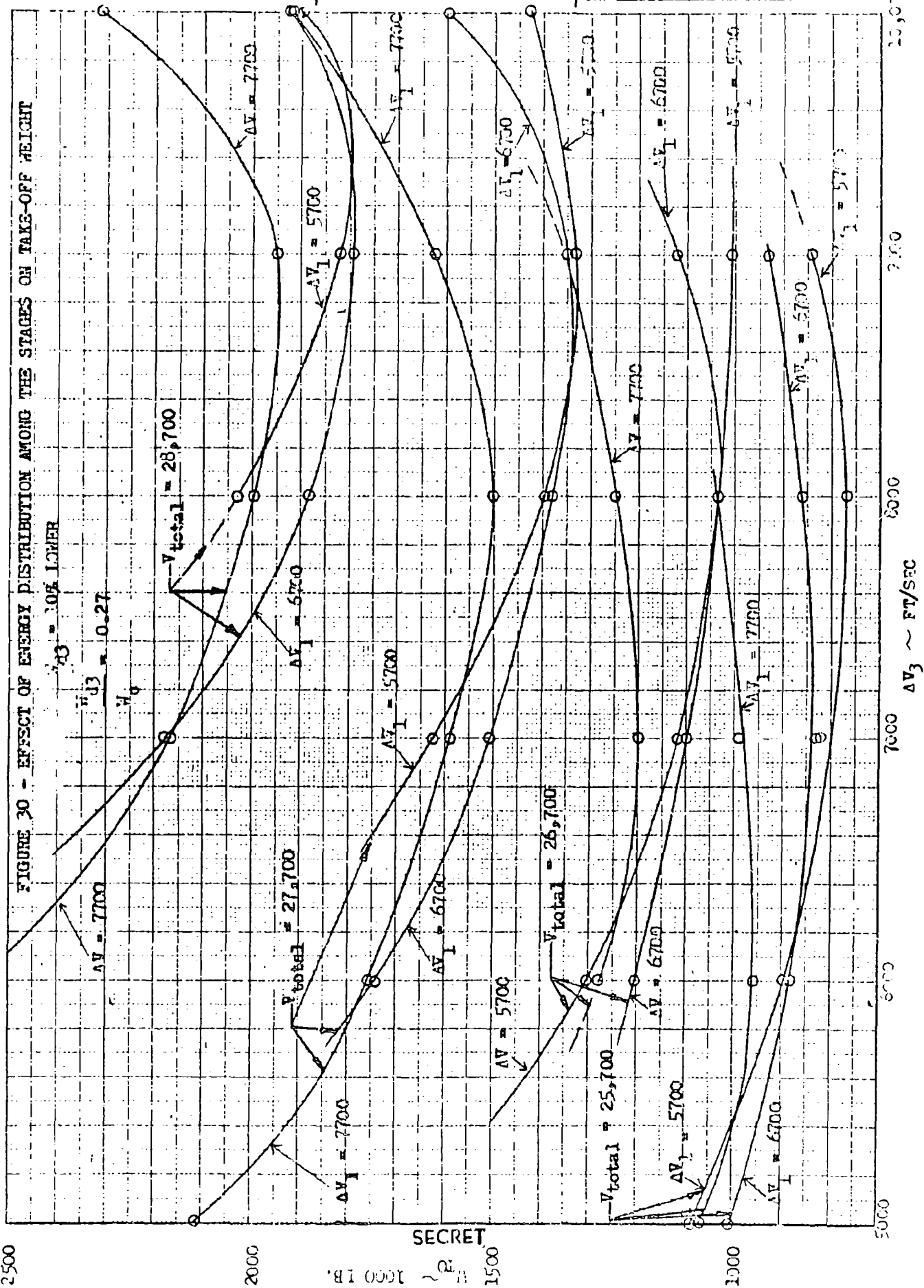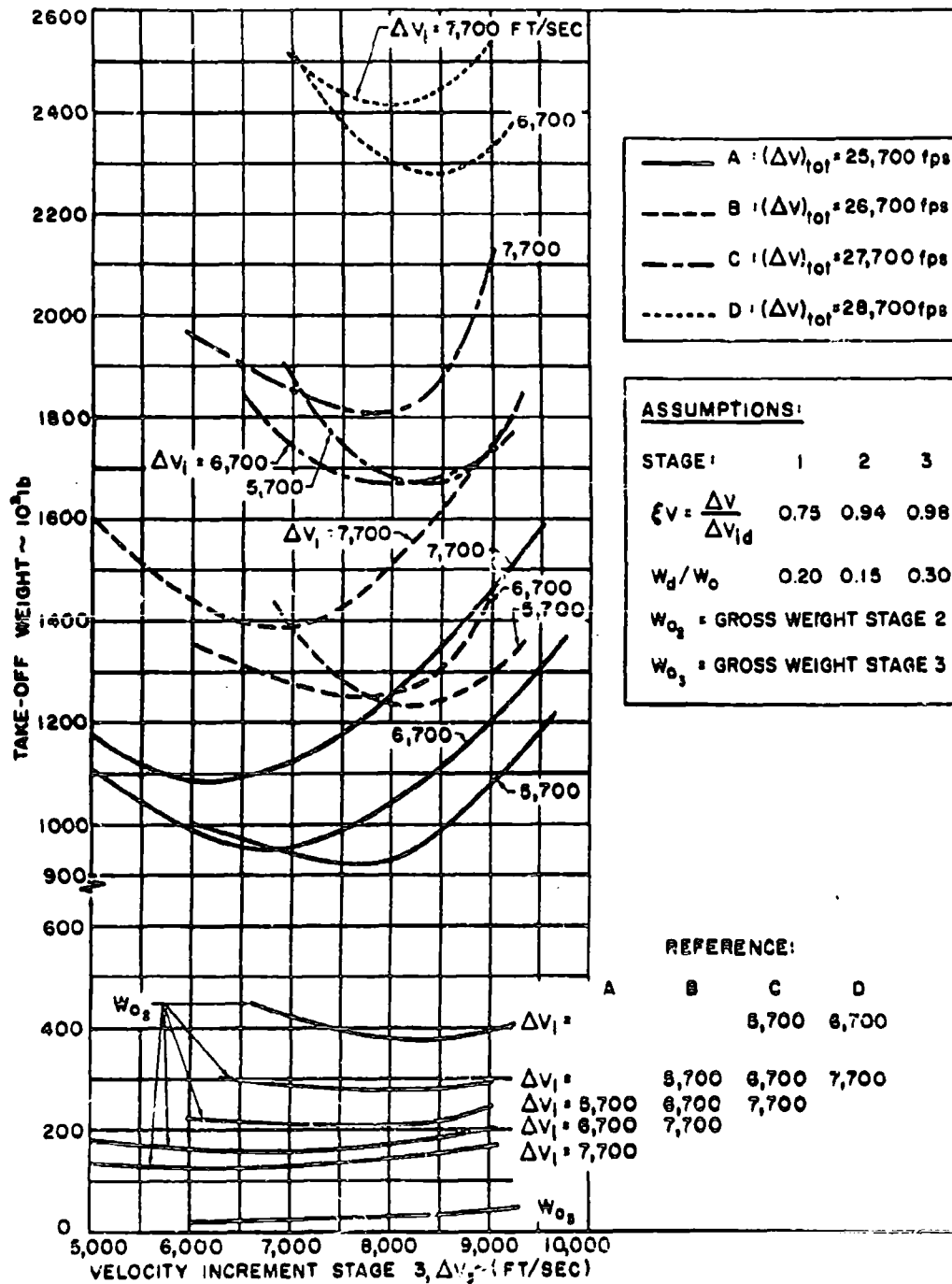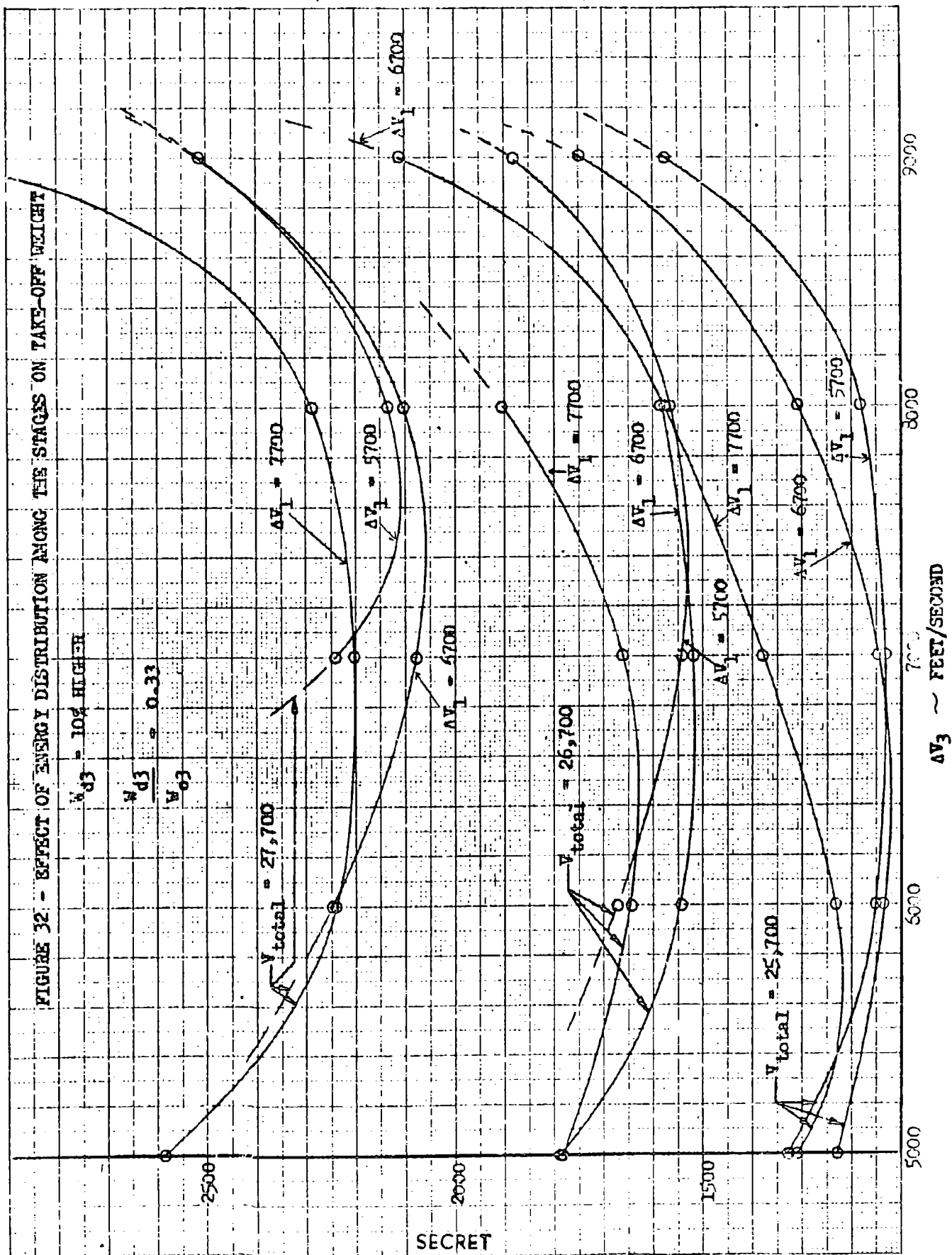Stages on Take-Off Weight

FIGURE 32 - EFFECT OF ENERGY DISTRIBUTION AMONG THE STAGES ON TAKE-OFF WEIGHT

By _____ Date _____

Checked _____ Date _____

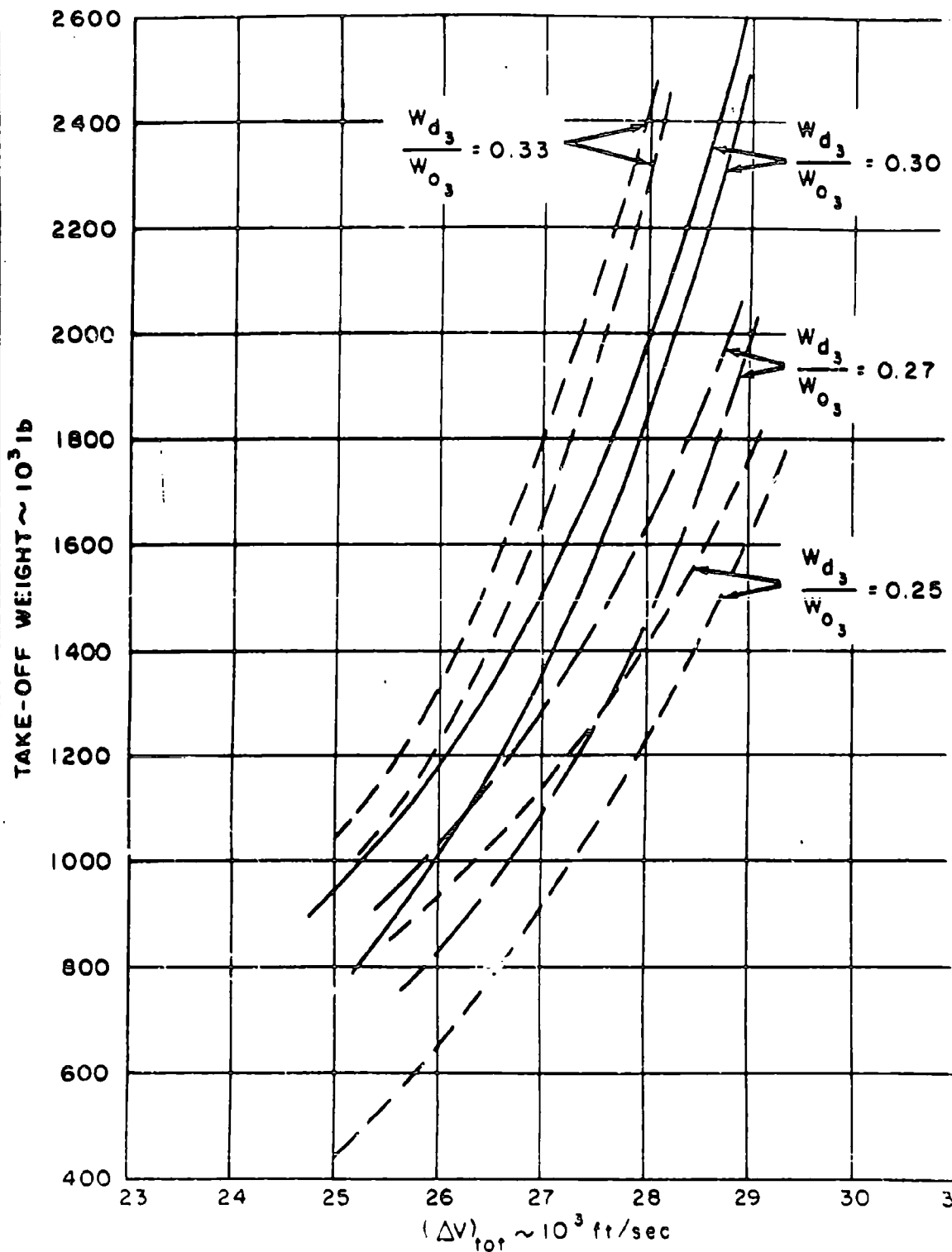**BELL** *Aircraft* CORPORATION

Model _____ Page __76__

Missile

Airplane _____ Report __D143-945-014__

Figure 33. Take-Off Weight as a Function of Cut-Off Velocity

By _____ _____ Date _____
Checked _____ Date ___
BELL Aircraft CORPORATION
Model _____ Page 77
Missile
Airplane _____ Report D143-945-014

the third stage. The limits of each band represent the values found for the "upper minimum" and the "lower minimum" for each set of three different stage velocity distributions such as shown in Figures 30 through 32. The effect of the third stage W_d/W_o ratios on the take-off weight is indicated in Figure 34 for four different cut-off velocities.

Accepting a dry weight to gross weight ratio of 0.3 for a winged third stage as a reasonable approximation, it can be seen that for the spiral path a take-off weight of the global weapon system of 920,000 to 1,000,000 pounds can be expected.

For the sustained path with circular velocity, the primary energy requirement is the same as for the spiral path. The additional energy requirement depends on the number of revolutions as well as on the exact cruising altitude. The velocity increment is given by $\Delta v_s = g_{oo}$ nt, values of which can be taken from Table I and the preceding list of t_r as a function of altitude (following Equation 54). Figure 35 shows the sustainer velocity increments Δv_s for one revolution and $C_D = 0.7$. For any other value C_D', the shown values must be multiplied by C_D'/C_D and for i revolutions the values must be multiplied by i. It is apparent that for a flight altitude above 500,000 feet, several revolutions would be required in order to increase the vehicle take-off weight greatly over that obtained for the spiral path. On the other hand, for 400,000 feet and below, the energy requirement for the sustained path becomes staggering. At 450,000 feet Δv_s is still 550 feet per second. For two revolutions (one sustained, the other gliding) it is therefore apparent that the sustained path does not require an appreciable increase in take-off weight. However, for more revolutions i.c., more than one sustained revolution, an altitude above 450,000 feet probably will have to be selected.

Figure 34 indicates the great effect of a reduction of Stage 3 gross weight W_{o3} on the over-all take-off weight W_{o1}. Since the over-all energy requirements for all types of global paths and even for a combined sustained-gliding MX-2276 with near-global capacity are all at $\Delta v_{id} \geq 29,000$ feet per second, the most important measure for reducing W_{o1}, is, apart from increase in I_{sp}, a decrease in W_{o3}. This can be done effectively only by removing the wings from this stage and treating it as a hypersonic glider rather than a more or less conventional airplane for which good landing qualities are important. These lead to requirements which are in agreement with good low-speed-operational requirements (especially, high). For the Stage 3 good flight qualities can be maintained even if , because of the independence of flight
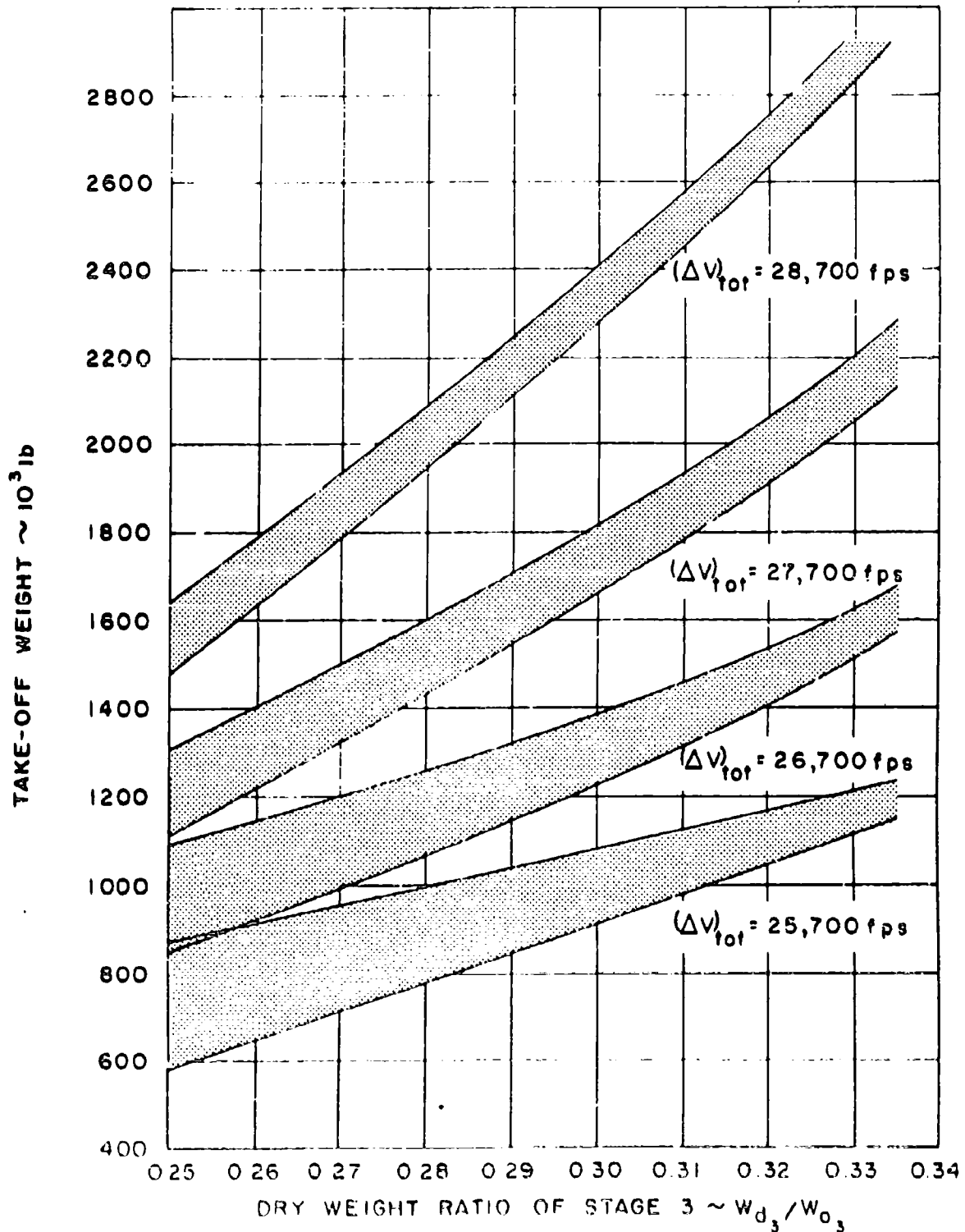
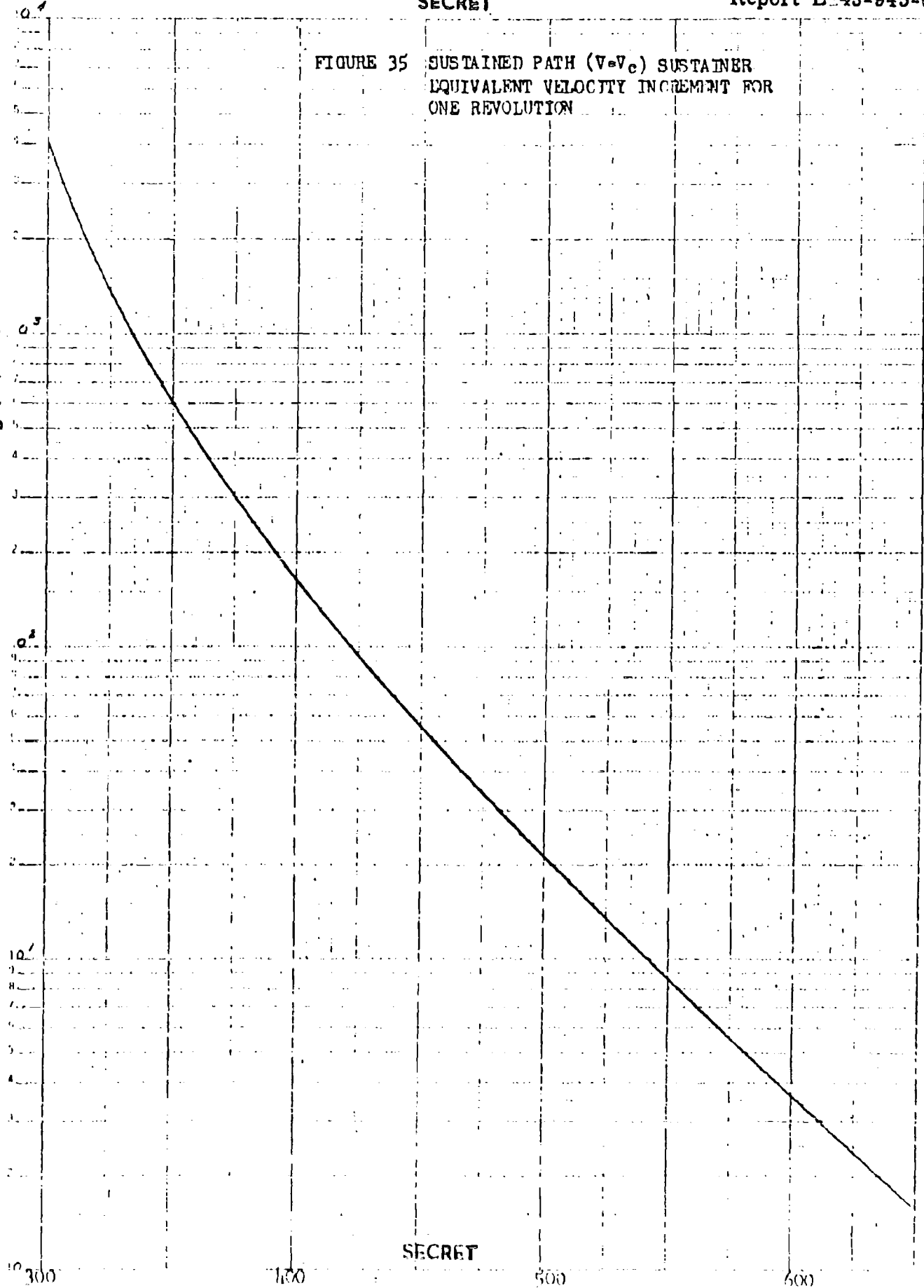Figure 34. Influence of Dry Weight Ratio of Stage 3 on
Take-Off Weight at Different Cut-Off Velocities

FIGURE 35 SUSTAINED PATH (V≈V_c) SUSTAINER
EQUIVALENT VELOCITY INCREMENT FOR
ONE REVOLUTION

ALTITUDE ~ 1000 FT.

By _____ Date _____

Checked _____ Date _____

BELL Aircraft CORPORATION

Model _____ Page 8C

Missile
Airplane _____ Report D143-945-014

qualities from planform configurations at hypersonic and high supersonic flow. Permitting bad landing qualities or eliminating conventional landing will, therefore, not only leave the good high-speed flight qualities un-affected, but, in addition, will cause a substantial reduction in structural weight (hence, in gross weight) of the upper stage. Reduction in bending moments alone, by going from the present MX-2276 planform to a "chisel" or "surfboard"-type body appears to make it possible to reduce the structural weight appreciably.

Of course, since the vehicle carries a pilot it is necessary to provide for some form of landing capability. This can be accomplished by equipping the vehicle with a parachute. It is visualized that Stage 3 glides to as low a velocity as possible until, at some subsonic speed, the stalling point is reached. Thereafter the parachute is released to accomplish the final descent to the surface. Low lifting area load will permit high equilibrium altitudes until the release of the parachute at subsonic speeds. The low-aspect ratio body-surface can operate at high angles of attack (25 to 35 degrees) to produce considerable lift (although a very bad L/D which, however, is not important here). The parachute can be expected to be comparatively light, because it has to function at subsonic speeds only.

If, taking this additional equipment into account, $(W_d/W_o)_3$ is re-duced from 0.3 to 0.25 (that is, only 1/6), the weight is reduced from 1.4 x 10^6 to 10^6 pounds (for Δv_{tot} = 26,700 feet per second) or from 10^6 pounds to 750,000 pounds for Δv_{tot} = 25,700 feet per second.

This reduction in take-off weight is considerable and will justify a more detailed investigation of this suggestion.

XI. CONCLUSIONS

It is not yet possible to single out the best path. However, this preliminary analysis has shown that the very high energy requirement for the constrained path is a serious disadvantage which necessarily must lead to larger vehicle take-off weights than in the other cases, or else to a severe restriction in payload capacity. The elliptic path is particularly sensitive to inaccuracies in cut-off velocity and cut-off angle and requires skillful operation at the apogee in order to enter the perigee at the correct altitude. Therefore, the elliptic path will require an advanced guidance, attitude control, and navigation system.

This leaves the spiral path and the sustained path, or a combination of these two as being of greatest immediate interest. It has been found in Section V, on the basis of the Rand atmosphere data as well as plausible, though perhaps somewhat conservative assumptions regarding the drag coefficient, that for one circumnavigation the spiral path requires an initial altitude of at least 400,000 feet. For the same altitude, two circumnavigations, one sustained and the second gliding (spiral) requires 2,455 pounds (cf. Table I, W_1 = 15,000 pounds, C_D = 0.7) of propellant in excess of what is needed for 1 spiral revolution (unpowered glide). It is obviously possible to reduce the initial altitude somewhat, to use a sustained path at circular velocity for 1/4 or 1/3 of the circumference, and then to enter the spiral path. Such combinations should be investigated, although, on the basis of the present results, not too much hope should be attached to them for finding a strikingly superior solution, because of the very bad lift/drag ratios under the flight conditions between 360,000 and 400,000 feet (essentially free molecule flow), and because of the rapidly increasing deceleration below 400,000 feet.

XII. RECOMMENDATIONS

For additional, more detailed flight path investigations it appears justified to recommend especially the following studies:

1. More detailed computation of initial altitude-range relations for the spiral path.

2. Additional investigations of the sustained path to determine data such as given in Tables I through III for specific vehicle weights, with emphasis to be placed on engine operation with continuously reducing thrust and its effect on the weight and complexity of the rocket engine assembly. Also the effect of the operational altitude should be studied further.

3. Investigation of the relative merits of a combined sustained-spiral path for one circumnavigation at a somewhat lower altitude than possible for either one spiral circumnavigation or one sustained circumnavigation plus one subsequent spiral circumnavigation.

4. Investigation of the feasibility of increasing the range of MX-2276 to global or reasonably near-global capacity (perhaps something like 18,000 to 19,000 nautical miles) so as to locate the landing site closer to the continental United States, thereby facilitating and expediting the return of Stage 3 to the launching site and to become independent of more remote countries in establishing landing sites for the MX-2276.

SECRET

Date ———
cked ——— Date ———

BELL Aircraft CORPORATION

Model ——— Page ——
Missile
Airplane ——— Report D143-945-014

XIII. REFERENCES

1. Grimminger, G.: "Analysis of Temperature, Pressure and Density of the Atmosphere, Extending to Extreme Altitudes": Rand Corporation Report No. R-105 dated 1 November 1948.

2. "Handbook of Supersonic Aerodynamics": Nav Ord Report No. 1488, Vol. 1, dated 1 April 1950.

3. Ashley, H.: "Applications of the Theory of Free Molecule Flow to Aeronautics": Institute of the Aeronautical Sciences, Preprint No. 164.

4. "Strategic Weapon System: Preliminary Design Report": Bell Aircraft Corporation Report No. D143-945-010, dated 15 July 1953.

5. "Flight Mechanics of a Satellite Rocket": Project Rand Report No. RA15021, dated February 1947.

6. Ehricke, K.: "Ascent of Orbital Vehicles" Bell Aircraft Corporation Report No. 02-981-017, dated 20 May 1954.

7. Ehricke, K.: "Preliminary Weight Studies on Multi-Stage Rocket Bomber of Given Performance": Bell Aircraft Corporation (Unpublished Report).

8. "Advanced Strategic Weapon System, Progress Report No. 6": Bell Aircraft Corporation Report No. D143-981-006, dated 15 November 1954.

Form E4-1 Rev. 353

17 March 2006

88 CG/SCCMF
3810 Communications Blvd
Wright-Patterson AFB OH 45433-7802

Defense Technical Information Center
Attn: Ms. Kelly Akers (DTIC-R)
8725 John J. Kingman Rd, Suite 0944
Ft Belvoir VA 22060-6218

Dear Ms. Akers,

   This concerns Technical Report AD073756, MX-2276 Advanced Strategic
Weapon System. Preliminary Global System Study, 28 April 1955. This technical
report, previously Unclassified/Limited Distribution, is now releasable to the
public. The attached AFMC Form 559 verifies that it was reviewed by release
authorities at Air Force Research Lab Air Vehicles Directorate (AFRL/VA) and
determined to be fully releasable to the public.

   Please call me at (937) 522-3091 if you have any questions.

                                        Sincerely

                                        Lynn Kane
                                        Freedom of Information Act Analyst
                                        Management Services Branch
                                        Base Information Management Division

Attachment
AFMC Form 559, RUSH – Freedom of Information Act